

Game-Theoretic Mixed H_2/H_∞ Control with Sparsity Constraint for Multi-agent Networked Control Systems

Feier Lian, Aranya Chakraborty *Senior Member, IEEE*, and Alexandra Duel-Hallen *Fellow, IEEE*

Abstract

Multi-agent networked control systems (NCSs) are often subject to model uncertainty and are limited by large communication cost, associated with feedback of data between the system nodes. To provide robustness against model uncertainty and to reduce the communication cost, this paper investigates the mixed H_2/H_∞ control problem for NCS under the sparsity constraint. First, proximal alternating linearized minimization (PALM) is employed to solve the centralized social optimization where the agents have the same optimization objective. Next, we investigate a sparsity-constrained noncooperative game, which accommodates different control-performance criteria of different agents, and propose a best-response dynamics algorithm based on PALM that converges to an approximate Generalized Nash Equilibrium (GNE) of this game. A special case of this game, where the agents have the same H_2 objective, produces a partially-distributed social optimization solution. We validate the proposed algorithms using a network with unstable node dynamics and demonstrate the superiority of the proposed PALM-based method to a previously investigated sparsity-constrained mixed H_2/H_∞ controller.

Index Terms

sparse controller, H_2 and H_∞ control, Linear Matrix Inequality (LMI), model uncertainty, nonconvex nonsmooth optimization, game theory

arXiv:1906.05562v1 [eess.SY] 13 Jun 2019

Game-Theoretic Mixed H_2/H_∞ Control with Sparsity Constraint for Multi-agent Networked Control Systems

I. INTRODUCTION

Recent research on multi-agent networks has proposed various methods for reducing communication cost for control by using sparse H_2 control designs [1]–[6]. However, most of this work ignores the effects of model uncertainties, which are bound to arise in most practical large-scale systems since the network operating conditions and topology change frequently over time. Even if the topology is fixed, the exact model parameters are not always available to the designer. The sparse control design in such cases must also be robust against the uncertainties. Robust designs have been reported in several recent papers such as [7]–[10] using H_∞ control, which is suitable for handling norm-bounded uncertainties in the system dynamics. In particular, [8], [9] employ both H_2 and H_∞ control, thus balancing the H_2 performance of the nominal system and robustness objective. However, optimizing the H_2 performance under the H_∞ and sparsity constraints has not been investigated by other researchers. Moreover, while a global control performance cost was optimized, this metric did not address the individual objectives of multiple agents under uncertainty.

Control of NCS under uncertainties has received significant attention recently in various domains, such as wide-area control of power systems [2], multi-robot coordination, multi-access broadcast channel, vehicle formation, and wireless sensor networks [11], [12]. In these problems, game theory becomes a powerful tool, with different control inputs modeled as game players, where each player aims to optimize its individual objective using an associated control policy. Differential games have been investigated for uncertain multi-agent systems, and algorithms for finding an equilibrium point have been proposed based on solving a set of coupled optimization problems. The works [13], [14] extend Nash-type differential game in [15] by finding robust Nash strategies while either considering polytopic uncertainty or formulating uncertain external disturbance as a fictitious player. The works [16]–[19] model the uncertainty using stochastic differential equations, and the Nash strategies are found by solving cross-coupled matrix equations through necessary optimality conditions or Karush-Kuhn-Tucker (KKT) conditions. Recently, reinforcement learning has been applied to multi-agent control Nash games when the system parameters are completely or partially unknown [20]–[23]. However, these reported game-theoretic designs did not address any sparsity constraint.

In this paper, we investigate controller designs for multi-agent systems that aim to reduce H_2 cost under H_∞ and

sparsity constraints. Both social optimization and a nonconvex game, where the H_2 -objectives of the agents are same and different, respectively, are investigated. We model our uncertainty as a norm-bounded parametric uncertainty that translates into an H_∞ constraint as in [9], [24]. We employ the proximal alternating linearized minimization (PALM) [5], which has been shown to be effective for optimization for nonconvex nonsmooth problems [25] and was utilized in [5] in a sparsity-constrained output-feedback co-design problem. First, a centralized sparsity-constrained mixed H_2/H_∞ controller, which represents the social optimization, is addressed. Preliminary results on this topic were recently reported in our conference paper [24], where we developed a centralized controller under the sparsity and H_∞ constraints using a greedy gradient support pursuit (GraSP) method [26]. However, the algorithm in [24] requires the knowledge of an initial stabilizing feedback gain that satisfies the sparsity constraint. We eliminate this requirement and show the advantages of the PALM-based controller in this paper over that in [24] in terms of the quadratic H_2 -cost.

Next, we extend the proposed design to the multi-agent scenario where each agent designs its own part of the feedback matrix, subject to a shared global H_∞ -norm and sparsity constraints. Since each agent has different individual cost, the control design is modeled as a noncooperative game with shared constraints. We develop a numerical algorithm to find the Generalized Nash Equilibrium (GNE) [27] of this game. The proposed algorithm has partially-distributed computation, i.e., in the first stage, each player computes its own feedback matrix while in the second stage, the sparse links are chosen globally based on the results from the first stage. Third, assuming all players of the game have the same H_2 -optimization objective, we develop a potential game that yields a partially-distributed implementation of the social optimization. We perform numerical simulations to demonstrate the performance of the proposed algorithms and discuss their convergence properties.

The main contributions of the paper can, therefore, be summarized as:

- Development and analysis of a centralized, sparsity-constrained mixed H_2/H_∞ controller for social optimization of multi-agent systems with norm-bounded uncertainty.
- Development of game-theoretic, partially-distributed algorithms that aim to minimize the H_2 -norms of the agents' transfer functions under shared sparsity and H_∞ -norm constraints.

TABLE I: Notation

Term	Definition
$\mathbf{M} > 0 (\succeq 0)$	Matrix \mathbf{M} is positive definite (semidefinite)
$\mathbf{M} < 0 (\preceq 0)$	\mathbf{M} is negative definite (semidefinite)
$\sigma_{\max}(\mathbf{M})$	maximum singular value of \mathbf{M}
$\ \mathbf{K}\ _F$	Frobenius norm of the matrix \mathbf{K} , defined by $\sqrt{\text{trace}(\mathbf{K}^T \mathbf{K})}$.
card(\mathbf{K})	Cardinality of matrix \mathbf{K} , defined by the number of nonzero elements in \mathbf{K} .
$\nabla_{\mathbf{K}} J(\mathbf{K})$	The gradient of the scalar function $J(\mathbf{K})$ with respect to the matrix \mathbf{K} . Assuming $\mathbf{K} \in \mathbb{R}^{m \times n}$, $\nabla_{\mathbf{K}} J(\mathbf{K})$ is given by a $m \times n$ matrix with the elements $[\nabla_{\mathbf{K}} J(\mathbf{K})]_{ij} = \partial J / \partial K_{ij}$.
$[\mathbf{K}]_s$	The matrix obtained by preserving only the s largest-magnitude entries of the matrix \mathbf{K} and setting all other entries to zero.
H_2 norm	The system H_2 norm in the time domain is $\ G\ _2 = (\int_0^\infty [\text{trace}(H(t)^T H(t))] dt)^{1/2}$, where $H(t)$ is the impulse response of the system.
H_∞ norm	The system H_∞ norm $\ G\ _\infty = \sup_\omega \sigma_{\max}(G(j\omega))$, where $G(j\omega)$ is the system transfer matrix.

The rest of the paper is organized as follows. Section II presents the system model with parametric uncertainty and develops a centralized PALM algorithm for social optimization using sparsity-constrained mixed H_2/H_∞ control. Section III describes a multi-agent system with parametric uncertainty, proposes a noncooperative game with shared sparsity and H_∞ constraints, and develops partially-distributed numerical algorithms for this game and for social optimization. Section IV demonstrates effectiveness of the proposed algorithms using numerical simulations, and discusses their complexities and convergence properties. Section V discusses future directions and concludes the paper.

Throughout the paper, matrices are denoted with boldface capital letters. If \mathbf{M} is a symmetric matrix, the upper block matrices are sometimes denoted by $*$ to save space. Some notation used is summarized in Table I.

II. PALM ALGORITHM FOR CENTRALIZED SPARSITY-CONSTRAINED MIXED H_2/H_∞ CONTROL

A. System model and mixed H_2/H_∞ control

Consider the following linear time-invariant system with model uncertainty:

$$\begin{aligned} \dot{\mathbf{x}}(t) &= \underbrace{(\mathbf{A} + \Delta\mathbf{A})}_{\hat{\mathbf{A}}} \mathbf{x}(t) + \underbrace{(\mathbf{B} + \Delta\mathbf{B})}_{\hat{\mathbf{B}}} \mathbf{u}(t) + \mathbf{B}_2 \mathbf{w}_2(t) \\ \mathbf{z}_2(t) &= \mathbf{C}_2 \mathbf{x}(t) + \mathbf{D}_2 \mathbf{u}(t) + \mathbf{D}_{22} \mathbf{w}_2(t) \\ \mathbf{y}(t) &= \mathbf{C} \mathbf{x}(t), \end{aligned} \quad (1)$$

where $\mathbf{x}(t) \in \mathbb{R}^{n \times 1}$ is the state vector, $\mathbf{u}(t) \in \mathbb{R}^{m \times 1}$ is the control input vector, $\mathbf{w}_2(t) \in \mathbb{R}^{m_2 \times 1}$ is the exogenous input, $\mathbf{z}_2(t) \in \mathbb{R}^{p_2 \times 1}$ is the performance output, and $\mathbf{y}(t) \in \mathbb{R}^{p \times 1}$ is the measured output. The matrices \mathbf{A} and \mathbf{B} are the nominal values of the state and input matrices, respectively, while $\Delta\mathbf{A}$ and $\Delta\mathbf{B}$ model the respective uncertainties. We make the following assumptions:

Assumption 1: (i) The pair (\mathbf{A}, \mathbf{B}) is controllable, (\mathbf{C}, \mathbf{A}) is observable, $(\mathbf{C}_2, \mathbf{A})$ is observable.

(ii) $\Delta\mathbf{A}$ and $\Delta\mathbf{B}$ have the form [9]

$$[\Delta\mathbf{A} \ \Delta\mathbf{B}] = \mathbf{B}_1 \Delta\delta [\mathbf{C}_1 \ \mathbf{D}_1], \quad (2)$$

where $\mathbf{B}_1 \in \mathbb{R}^{n \times m_1}$, $\mathbf{C}_1 \in \mathbb{R}^{p_1 \times n}$, $\mathbf{D}_1 \in \mathbb{R}^{p_1 \times m}$ are known matrices, and $\Delta\delta \in \mathbb{R}^{m_1 \times p_1}$ is an unknown matrix which is norm-bounded, satisfying $\Delta\delta^T \Delta\delta \preceq 1/\gamma^2 \mathbf{I}$ for any scalar $\gamma > 0$.

Assumption 2: Matrices \mathbf{C}_2 and \mathbf{D}_2 have the following form:

$$\mathbf{C}_2 = [\mathbf{C}_2^1, \mathbf{0}], \mathbf{D}_2 = \begin{bmatrix} \mathbf{0} \\ \mathbf{D}_2^2 \end{bmatrix}, \mathbf{C}_2^T \mathbf{D}_2 = \mathbf{0}. \quad (3)$$

Using assumptions 1 and 2, the system (1) can be expressed as the feedback interconnection of the following two subsystems:

$$\Sigma : \begin{cases} \dot{\mathbf{x}}(t) = \mathbf{A} \mathbf{x}(t) + \mathbf{B} \mathbf{u}(t) + \mathbf{B}_1 \mathbf{w}_1(t) + \mathbf{B}_2 \mathbf{w}_2(t) \\ \mathbf{z}_1(t) = \mathbf{C}_1 \mathbf{x}(t) + \mathbf{D}_1 \mathbf{u}(t) \\ \mathbf{z}_2(t) = \mathbf{C}_2 \mathbf{x}(t) + \mathbf{D}_2 \mathbf{u}(t) + \mathbf{D}_{22} \mathbf{w}_2(t) \\ \mathbf{y}(t) = \mathbf{C} \mathbf{x}(t) \end{cases} \quad (4)$$

$$\Sigma_K : \begin{cases} \mathbf{w}_1(t) = \Delta\delta \mathbf{z}_1(t), \end{cases} \quad (5)$$

where $\mathbf{z}_1(t) \in \mathbb{R}^{p_1 \times 1}$, $\mathbf{w}_1(t) \in \mathbb{R}^{m_1 \times 1}$.

Our goal in this section is to find a linear static output-feedback controller $\mathbf{u}(t) = -\mathbf{K} \mathbf{y}(t)$ that stabilizes (1), i.e., guarantees $\|T_{z_1 w_1}(\mathbf{K})\|_\infty < \gamma$. Following [28], this H_∞ -norm constraint can be transformed into an Linear Matrix Inequality (LMI) condition as stated in the following theorem.

Theorem 1: The H_∞ -norm constraint $\|T_{z_1 w_1}(\mathbf{K})\|_\infty < \gamma$ holds if and only if there exists an $\mathbf{X} = \mathbf{X}^T$ that satisfies the LMI

$$\begin{bmatrix} \mathbf{A}_{cl}(\mathbf{K}) \mathbf{X} + \mathbf{X} \mathbf{A}_{cl}(\mathbf{K})^T + \mathbf{B}_1 \mathbf{B}_1^T & \mathbf{X} \mathbf{C}_{cl1}(\mathbf{K})^T \\ \mathbf{C}_{cl1}(\mathbf{K}) \mathbf{X} & -\gamma^2 \mathbf{I} \end{bmatrix} \prec 0 \quad (6)$$

$$\mathbf{X} \succ 0$$

where $\mathbf{A}_{cl}(\mathbf{K}) = \mathbf{A} - \mathbf{B} \mathbf{K} \mathbf{C}$, $\mathbf{C}_{cli}(\mathbf{K}) = \mathbf{C}_i - \mathbf{D}_i \mathbf{K} \mathbf{C}$ for $i = 1, 2$.

The **mixed H_2/H_∞ control problem** can then be stated as: Given an achievable H_∞ -norm bound γ , find a feedback controller $\mathbf{K} \in \mathbb{R}^{m \times p}$ that solves

$$\text{Minimize}_{\mathbf{K}} \|T_{z_2 w_2}(\mathbf{K})\|_2, \quad (7)$$

$$\text{s.t } \mathbf{u}(t) = -\mathbf{K} \mathbf{y}(t), \text{ equation (4) holds, and} \quad (8)$$

$$\|T_{z_1 w_1}(\mathbf{K})\|_\infty < \gamma \text{ (or equivalently, (6) holds).} \quad (9)$$

$T_{z_2 w_2}$ is the closed-loop transfer function from \mathbf{w}_2 to \mathbf{z}_2 .

For simplicity, and without loss of generality, we set $\mathbf{D}_{22} = \mathbf{0}$ in (1). Following standard robust control results, such as in [28], it can be shown that the squared H_2 norm from \mathbf{w}_2 to \mathbf{z}_2 for the system (4) is

$$\|T_{z_2 w_2}(\mathbf{K})\|_2^2 = J(\mathbf{K}) := \text{trace}(\mathbf{B}_2^T \mathbf{P} \mathbf{B}_2) \quad (10)$$

where \mathbf{P} is the solution of the Lyapunov equation

$$\mathbf{P} \mathbf{A}_{cl}(\mathbf{K}) + \mathbf{A}_{cl}(\mathbf{K})^T \mathbf{P} + \mathbf{C}_{cl2}(\mathbf{K})^T \mathbf{C}_{cl2}(\mathbf{K}) = \mathbf{0}. \quad (11)$$

We can define

$$\mathbf{Q} = (\mathbf{C}_2^1)^T \mathbf{C}_2^1 \succeq 0, \mathbf{R} = (\mathbf{D}_2^2)^T \mathbf{D}_2^2 \succ 0 \quad (12)$$

in which case the objective $J(\mathbf{K})$ in (10) can be written as

$$J(\mathbf{K}) = \int_{t=0}^{\infty} [\mathbf{x}^T(t) \mathbf{Q} \mathbf{x}(t) + \mathbf{u}^T(t) \mathbf{R} \mathbf{u}(t)] dt. \quad (13)$$

B. Sparsity-constrained mixed H_2/H_∞ control

The solution \mathbf{K} in problem (7)-(9) is usually a dense matrix, meaning that every sensor must send the sensed outputs to every controller. This can result in a large communication cost.

To reduce this cost, we impose a sparsity constraint on the feedback matrix [2], [24], resulting in the following sparsity-constrained mixed H_2/H_∞ problem:

$$\begin{aligned} \min_{\mathbf{K}} \quad & \|T_{z_2 w_2}(\mathbf{K})\|_2, \\ \text{s.t.} \quad & \|T_{z_1 w_1}(\mathbf{K})\|_\infty < \gamma, \quad \text{card}(\mathbf{K}) \leq s, \end{aligned} \quad (14)$$

with the plant model satisfying (4). For simplicity, we define each nonzero entry in \mathbf{K} as one communication link. Alternative definitions of sparsity and their effects on the actual cost of communication are discussed in [2].

C. Overview of the centralized PALM algorithm

The sparsity-constrained mixed H_2/H_∞ problem (14) was solved in our recent paper [24] using the GraSP algorithm, assuming that for any given value of s we can find an initial guess for \mathbf{K} that satisfies the s -sparse structure. Depending on the plant model and the uncertainty in (4), finding such a feasible initial guess in reality, however, can be quite difficult. In this section, we eliminate this requirement by introducing a sparsity-constrained optimization algorithm based on PALM. For this, we first transform (14) into a problem with two optimization variables, \mathbf{K} and \mathbf{F} , where \mathbf{K} is defined in (8), and \mathbf{F} represents the sparse feedback matrix that satisfies the cardinality constraint. The problem (14) can then be reformulated as follows:

$$\begin{aligned} \min_{\mathbf{K}, \mathbf{F}} \quad & J(\mathbf{K}) + \frac{\rho}{2} \|\mathbf{K} - \mathbf{F}\|_F^2, \\ \text{s.t.} \quad & \|T_{z_1 w_1}(\mathbf{K})\|_\infty < \gamma, \\ & \text{card}(\mathbf{F}) \leq s, \end{aligned} \quad (15)$$

where the penalty term $\rho/2 \|\mathbf{K} - \mathbf{F}\|_F^2$ is used to regularize the difference between \mathbf{K} and \mathbf{F} . When the parameter ρ is chosen large enough, this term can be reduced sufficiently. There are two constrained variables in (15). We next transform (15) to an unconstrained optimization problem by defining the following indicator functions:

$$g(\mathbf{K}) = \begin{cases} 0, & T_\infty(\mathbf{K}) < \gamma \\ +\infty, & \text{O.W.} \end{cases} \quad (16)$$

$$f(\mathbf{F}) = \begin{cases} 0, & \text{card}(\mathbf{F}) \leq s \\ +\infty, & \text{O.W.} \end{cases} \quad (17)$$

Using (16) and (17) the problem (15) can be written as

$$\min_{\mathbf{K}, \mathbf{F}} \Phi(\mathbf{K}, \mathbf{F}), \quad (18)$$

where

$$\Phi(\mathbf{K}, \mathbf{F}) = J(\mathbf{K}) + g(\mathbf{K}) + f(\mathbf{F}) + H(\mathbf{K}, \mathbf{F}) \quad (19)$$

with

$$H(\mathbf{K}, \mathbf{F}) = \frac{\rho}{2} \|\mathbf{K} - \mathbf{F}\|_F^2 \quad (20)$$

being the coupling function between \mathbf{K} and \mathbf{F} .

The PALM algorithm proceeds by alternating the minimization on the variables (\mathbf{K}, \mathbf{F}) through separate subproblems [25], which simplifies solving (18), as described below. When \mathbf{K} is fixed, the optimization (18) reduces to minimizing the sum of a nonsmooth function $f(\mathbf{F})$ and a smooth function $H(\mathbf{K}, \mathbf{F})$ of \mathbf{F} . From the result of proximal forward-backward splitting algorithm [25], minimizing $f + H$ can be relaxed as iteratively upper bounding the objective and minimizing the

upper bound [29]. The iteration can be written as

$$\mathbf{F}^{k+1} = \quad (21)$$

$$\arg \min_{\mathbf{F}} \left\{ \langle \mathbf{F} - \mathbf{F}^k, \nabla_{\mathbf{F}} H(\mathbf{F}, \mathbf{K}) \rangle + \frac{t}{2} \|\mathbf{F} - \mathbf{F}^k\|_F^2 + f(\mathbf{F}) \right\},$$

where $\langle \cdot, \cdot \rangle$ denotes inner product. Minimizing the first two terms is equivalent to minimizing the first order (linear) approximation of $H(\mathbf{K}, \mathbf{F})$ at $\mathbf{F} = \mathbf{F}^k$, regularized by a trust-region penalty near \mathbf{F}^k . When $t \in (L, \infty)$ and L is the Lipschitz constant (see S.II [30] and Appendix B.3 [31]) for $\nabla_{\mathbf{F}} H(\mathbf{K}, \mathbf{F})$, the regularized linear approximation provides an upper bound on $H(\mathbf{K}, \mathbf{F})$ [29].

Eq. (21) can be rewritten compactly using the definition of a proximal map as

$$\mathbf{F}^{k+1} \in \text{prox}_t^f(\mathbf{F}^k - 1/t \nabla_{\mathbf{F}} H(\mathbf{K}, \mathbf{F}^k)), \quad (22)$$

where for $\sigma: \mathbb{R}^d \rightarrow (\infty, \infty]$, a proper and lower semicontinuous function, $x \in \mathbb{R}^d$ and $t > 0$, the proximal map associated with σ at point \mathbf{x} is

$$\text{prox}_t^\sigma(\mathbf{x}) = \arg \min_{\mathbf{u} \in \mathbb{R}^d} \left\{ \sigma(\mathbf{u}) + \frac{t}{2} \|\mathbf{u} - \mathbf{x}\|^2 \right\}. \quad (23)$$

Similar analysis can be carried out for the minimization of (18) when \mathbf{F} is fixed. In summary, the PALM algorithm minimizes (18) by alternatively finding the proximal maps:

$$\mathbf{F}^{k+1} \in \text{prox}_{a_k}^f(\mathbf{F}^k - 1/a_k \nabla_{\mathbf{F}} H(\mathbf{K}^k, \mathbf{F}^k)) \quad (24)$$

$$\mathbf{K}^{k+1} \in \text{prox}_{b_k}^{J+g}(\mathbf{K}^k - 1/b_k \nabla_{\mathbf{K}} H(\mathbf{K}^k, \mathbf{F}^{k+1})) \quad (25)$$

where a_k and b_k are positive constants that are greater than the Lipschitz constants $L_1(\mathbf{K}^k)$ and $L_2(\mathbf{F}^{k+1})$ of $\nabla_{\mathbf{F}} H(\mathbf{K}^k, \mathbf{F})$ and $\nabla_{\mathbf{K}} H(\mathbf{K}, \mathbf{F}^{k+1})$, respectively.

D. Algorithm description

We summarize the PALM algorithm for sparsity-constrained mixed H_2/H_∞ control in Algorithm 1. In Steps 2 and 3 of Algorithm 1, \mathbf{F} -minimization (24) and \mathbf{K} -minimization (25) are performed, respectively. In Step 2, we perform iterative \mathbf{F} -minimization (24), which can be rewritten from (23) as:

$$\mathbf{F}^{k+1} = \arg \min_{\mathbf{F}} \left\{ f(\mathbf{F}) + \frac{a_k}{2} \|\mathbf{F} - \mathbf{Z}^k\|_F^2 \right\} \quad (26)$$

where \mathbf{Z}^k is the point within the parenthesis in (24), found in Step 2.2. It is easy to see that the partial gradients of $H(\mathbf{K}, \mathbf{F})$,

Algorithm 1 PALM algorithm for the mixed H_2/H_∞ control algorithm with sparsity constraint

Given s : sparsity constraint, γ : H_∞ -norm bound.

1. Initialization:

\mathbf{K}^0 : any stabilizing feedback gain with $T_\infty(\mathbf{K}^0) < \gamma$.

\mathbf{F}^0 : any stabilizing feedback gain \mathbf{F}^0 .

Compute $a := \gamma_1 \rho$, $b := \gamma_2 \rho$.

for $k = 1, 2, \dots, k_{\max}$ **until** $\|\mathbf{K}^{k+1} - \mathbf{K}^k\|_F < \epsilon_1$ **or** $\|\mathbf{F}^{k+1} - \mathbf{F}^k\|_F < \epsilon_2$ **do**

 // 2. \mathbf{F} -minimization step

 2.1 Compute $\mathbf{Z}^k := \mathbf{F}^k - \frac{1}{a} \nabla_{\mathbf{F}} H(\mathbf{K}^k, \mathbf{F}^k)$

 2.2 Prune \mathbf{Z}^k : $\mathbf{F}^{k+1} := [\mathbf{Z}^k]_s$.

 // 3. \mathbf{K} -minimization step

 3.1 Compute $\mathbf{X}^k := \mathbf{K}^k - \frac{1}{b} \nabla_{\mathbf{K}} H(\mathbf{K}^k, \mathbf{F}^{k+1})$.

 3.2 Update \mathbf{K}^{k+1} : $\mathbf{K}^{k+1} := \text{KPROXOP}(\mathbf{K}^k, \mathbf{X}^k, b)$.

end for

defined in (20) are

$$\begin{aligned}\nabla_{\mathbf{K}}H(\mathbf{K}, \mathbf{F}) &= \rho(\mathbf{K} - \mathbf{F}) \\ \nabla_{\mathbf{F}}H(\mathbf{K}, \mathbf{F}) &= \rho(\mathbf{F} - \mathbf{K}).\end{aligned}\quad (27)$$

From (27), the Lipschitz constant $L_1(\mathbf{K}^k) = \rho$, and thus the constant a_k in (24) and (26) is defined as

$$a_k = a = \gamma_1 \rho \quad (28)$$

with $\gamma_1 > 1$.

In Step 3 of Algorithm 1, we perform iterative \mathbf{K} -minimization:

$$\mathbf{K}^{k+1} = \arg \min_{\mathbf{K}} \left\{ J(\mathbf{K}) + g(\mathbf{K}) + \frac{b_k}{2} \|\mathbf{K} - \mathbf{X}^k\|_F^2 \right\}, \quad (29)$$

which is equivalent to (25), and b_k is chosen as $b_k = b = \gamma_2 \rho$, with $\gamma_2 > 1$.

In the following, we present the solutions for Eq. (26) and (29) used in Steps 2 and 3 of Algorithm 1.

1) **F-minimization:** Applying the proximal operator (24) of function f is equivalent to minimizing a regularized version of f . In (26), f is an indicator function of the set $\mathcal{X} = \{\mathbf{F} | \text{card}(\mathbf{K}) \leq s\}$ (17), so the proximal operator in (26) (Step 2.3 in Algorithm 1) is equivalent to the projection of Z^k onto the set \mathcal{X} . Therefore, we can rewrite (26) as

$$\begin{aligned}\mathbf{F}^{k+1} &= \arg \min_{\mathbf{F}} \|\mathbf{F} - \mathbf{Z}^k\|_F^2 \\ \text{s.t. } \text{card}(\mathbf{F}) &\leq s.\end{aligned}\quad (30)$$

As shown in [5], [25], the solution to (30) is $[\mathbf{Z}^k]_s$ (see Table I), which is Step 2.3 of Algorithm 1.

Algorithm 2 KPROXOP: Subroutine to solve (31)

```

1: procedure KPROXOP( $\mathbf{K}^{\text{cur}}, \mathbf{X}^k, b$ )
2:   while True do
3:      $\mathbf{K}^{\text{prev}} := \mathbf{K}^{\text{cur}}$ 
4:     if  $\|\nabla_{\mathbf{K}}h(\mathbf{K}^{\text{cur}})\|_F < \epsilon_3$  then
5:       // Stationary point in the interior of the  $H_\infty$ -
       // constraint set.
6:       break
7:     end if
8:     // Take a gradient-descent step in the interior of
     // the  $H_\infty$ -constraint set.
9:      $\mathbf{K}^{\text{cur}} := \mathbf{K}^{\text{prev}} - d\nabla_{\mathbf{K}}h(\mathbf{K}^{\text{prev}})$ , where step size
     //  $d > 0$  is chosen by backtracking line search [32] s.t.
     //  $T_\infty(\mathbf{K}^{\text{cur}}) < \gamma$ 
10:    if  $d < \epsilon_2$  then
11:      //  $\mathbf{K}^{\text{prev}}$  is near the boundary of the  $H_\infty$ -
      // constraint set
12:      Solve for  $\mathbf{K}^{\text{in}}$  using (36). Let  $\Delta\mathbf{K}^{\text{cur}} := \mathbf{K}^{\text{in}} -$ 
      //  $\mathbf{K}^{\text{prev}}$ .
13:       $\mathbf{K}^{\text{cur}} := \mathbf{K}^{\text{prev}} + d'\Delta\mathbf{K}^{\text{cur}}$ , where  $d'$  is deter-
      // mined by backtracking line search [32].
14:    end if
15:    if  $\|\mathbf{K}^{\text{cur}} - \mathbf{K}^{\text{prev}}\|_F < \epsilon_1$  then
16:      break
17:    end if
18:  end while
19: end procedure

```

2) **K-minimization:** Next we focus on the proximal operator for (29), which is equivalent to

$$\begin{aligned}\min_{\mathbf{K}} h(\mathbf{K}) \\ \text{s.t. } T_\infty(\mathbf{K}) < \gamma\end{aligned}\quad (31)$$

where

$$h(\mathbf{K}) \triangleq \left(J(\mathbf{K}) + \frac{b_k}{2} \|\mathbf{K} - \mathbf{X}^k\|_F^2 \right). \quad (32)$$

We propose to solve (31) using a feasible direction method in the search space of \mathbf{K} , summarized in Algorithm 2. Starting from an interior point of the feasible region of the problem (In step 3.2 of Algorithm 1, \mathbf{K}^k always satisfies $T_\infty(\mathbf{K}^k) < \gamma$), the algorithm first descends along the gradient of $h(\mathbf{K})$ until the solution reaches a stationary point in the interior (line 6) or on the boundary of the constraint set. When the solution is in the interior of the feasible region, a gradient-descent update step is used (line 9). When the current solution is at the boundary and the gradient-descent direction violates the H_∞ -norm constraint, we seek a direction that reduces the minimization objective and simultaneously moves the solution away from the boundary of the H_∞ -norm constraint set to its interior (lines 12-13 in Algorithm 2).

In lines 12-13, we find the improving feasible direction for (31) when the solution is at the boundary of the feasible region. We recall the Zoutendijk's method [33] as the foundation for general feasible direction methods, which requires evaluating the gradients of both the objective and the constraint functions, i.e., $\nabla_{\mathbf{K}}h(\mathbf{K})$ and $\nabla_{\mathbf{K}}T_\infty(\mathbf{K})$. In the original formulation of Zoutendijk's method (S.I [30], Appendix B.2 in [31]), the gradient of the constraint function is evaluated to form conditions for the improving feasible direction. However, due to the difficulty in evaluating the gradient of an H_∞ norm, we utilize the concept of level sets as in [34], as well as their LMI interpretation, to develop an alternative condition.

In each step of the Zoutendijk's method, a linear programming subproblem is solved to find the improving feasible direction. The inequality $\text{trace}[(\nabla_{\mathbf{K}}h(\mathbf{K}))^T \cdot \Delta\mathbf{K}] < 0$ guarantees that an update direction $\Delta\mathbf{K}$ decreases $h(\mathbf{K})$ in (31). Moreover, the inequality which involves gradient of the H_∞ norm, i.e., $\text{trace}[(\nabla_{\mathbf{K}}\|T_{z_1 w_1}(\mathbf{K})\|_\infty)^T \cdot \Delta\mathbf{K}] < 0$ can be used to check if $\Delta\mathbf{K}$ moves away from the H_∞ bound. In the gain space of $\mathbf{K} \in \mathbb{R}^{m \times n}$, the set of all stabilizing \mathbf{K} which satisfy (6), i.e., with H_∞ norm smaller than γ , is a level set

$$\mathcal{K}(\gamma) := \{\mathbf{K} | \|T_{z_1 w_1}(\mathbf{K})\|_\infty < \gamma\}. \quad (33)$$

Given a stabilizing gain \mathbf{K}^0 , the algorithm in [34] proceeds by first finding a sufficiently small γ_0 such that $\mathbf{K}^0 \in \mathcal{K}(\gamma_0)$. Next, a convex subset $\hat{\mathcal{K}}(\gamma_0)$ of $\mathcal{K}(\gamma_0)$, which also contains \mathbf{K}^0 near the boundary, can be formed using an LMI sufficient condition. Then an inner point \mathbf{K}^{in} of $\hat{\mathcal{K}}(\gamma_0)$ is found using the following sufficient LMI condition.

For the above (\mathbf{K}^0, γ_0) , \mathbf{K}^{in} is an inner point of $\hat{\mathcal{K}}(\gamma_0)$ if the matrix function $\mathbf{G}(\mathbf{K}^{\text{in}}; \mathbf{K}^0)$ is positive definite, i.e.,

$$\mathbf{G}(\mathbf{K}^{\text{in}}; \mathbf{K}^0) \succ 0 \Rightarrow \mathbf{K}^{\text{in}} \in \hat{\mathcal{K}}(\gamma_0). \quad (34)$$

The details of computing $\mathbf{G}(\mathbf{K}^{\text{in}}; \mathbf{K}^0)$ are provided in [24].

We combine the LMI condition (34) and the gradient of $h(\mathbf{K})$ in (31) to form the iterative algorithm for solving (31).

The gradient of $h(\mathbf{K})$ is

$$\nabla_{\mathbf{K}} h(\mathbf{K}) = 2(\mathbf{R}\mathbf{K}\mathbf{C} - \mathbf{B}^T \mathbf{P})\mathbf{L}\mathbf{C}^T + b_k(\mathbf{K} - \mathbf{X}^k). \quad (35)$$

Thus, given a current solution \mathbf{K}^{cur} near the boundary of the H_∞ -norm constraint set, an improving feasible point \mathbf{K}^{in} can be found by solving the following linear matrix inequality:

$$\begin{aligned} \max_{z, \mathbf{K}^{\text{in}}} \quad & z \\ \text{s.t.} \quad & \text{trace}[(\nabla_{\mathbf{K}} h(\mathbf{K}^{\text{cur}}))^T (\mathbf{K}^{\text{in}} - \mathbf{K}^{\text{cur}})] + z \leq 0 \\ & \mathbf{G}(\mathbf{K}^{\text{in}}; \mathbf{K}^{\text{cur}}) - \theta z \cdot \mathbf{I} \succeq 0. \end{aligned} \quad (36)$$

The parameter $\theta \geq 0$ is a predetermined factor that controls how far \mathbf{K} moves away from the H_∞ -norm boundary. The value of θ determines the speed of reduction of the H_∞ norm, with a small value of θ resulting in a less aggressive shrinkage of the H_∞ norm. If the solution z^* in (36) is positive, then $\mathbf{K}^{\text{in}} - \mathbf{K}^{\text{cur}}$ is an improving feasible direction; otherwise, an improving feasible direction cannot be found.

Given the current solution \mathbf{K}^{cur} and the inner point \mathbf{K}^{in} solved in (36), the update rule is given in lines 12–13 of Algorithm 2, where $d' \leq 1$ is the step size found by a backtracking line search using the Armijo condition [33].

III. SPARSITY-CONSTRAINED NONCOOPERATIVE GAMES FOR MULTI-AGENT CONTROL

A. Multi-agent model and generalized Nash equilibrium

Next, we extend the optimization in Section II to the case when the agents have different optimization objectives. To accommodate this scenario, we consider the following multi-agent system with model uncertainty in \mathbf{A} and \mathbf{B} matrices. Consider a network of N agents, where agent i employs its control strategy $\mathbf{u}_i(t) \in \mathbb{R}^{q_i \times 1}$, $i = 1, \dots, N$. Thus, (1) becomes

$$\begin{aligned} \dot{\mathbf{x}}(t) &= (\mathbf{A} + \Delta\mathbf{A})\mathbf{x}(t) + \sum_{i=1}^N (\mathbf{B}_{(i)} + \Delta\mathbf{B}_{(i)}) \mathbf{u}_i(t) + \mathbf{B}_2 \mathbf{w}_2(t) \\ \mathbf{y}(t) &= \mathbf{C}\mathbf{x}(t) \\ \mathbf{u}_i(t) &= -\mathbf{K}_i \mathbf{y}(t), \quad i = 1, \dots, N, \end{aligned} \quad (37)$$

where $\mathbf{A} \in \mathbb{R}^{n \times n}$, $\mathbf{B}_{(i)} \in \mathbb{R}^{n \times q_i}$ represent the nominal values of the state and control matrix, respectively, for the i -th control input. We assume all agents know \mathbf{A} and $\mathbf{B}_{(i)}$ for $i = 1, \dots, N$, and the uncertain matrices $\Delta\mathbf{A} \in \mathbb{R}^{n \times n}$ and $\Delta\mathbf{B} \triangleq [\Delta\mathbf{B}_{(1)}, \Delta\mathbf{B}_{(2)}, \dots, \Delta\mathbf{B}_{(N)}]$ satisfy the norm-bounded assumption (2), where $\Delta\mathbf{B}_{(i)} \in \mathbb{R}^{q_i \times n}$. Note that $\mathbf{B}_{(i)}$ is the column block of \mathbf{B} in (1), with $\sum_{i=1}^N \mathbf{B}_{(i)} \mathbf{u}_i = \mathbf{B}\mathbf{u}$, and $\mathbf{K}_i \in \mathbb{R}^{q_i \times p}$ is the row block of \mathbf{K} in (8) associated with the rows corresponding to the control inputs for agent i . Thus, the multi-agent system can be expressed in the form (4–5), with the first equation in (4) replaced by

$$\dot{\mathbf{x}}(t) = \mathbf{A}\mathbf{x}(t) + \sum_{i=1}^N \mathbf{B}_{(i)} \mathbf{u}_i(t) + \mathbf{B}_1 \mathbf{w}_1(t) + \mathbf{B}_2 \mathbf{w}_2(t). \quad (38)$$

We introduce the following notation. Let \mathbf{K}_{-i} denote the set of strategies $j \neq i, j = 1, \dots, N$. When agent i chooses its strategy \mathbf{K}_i in (37) given \mathbf{K}_{-i} , we refer to the resulting feedback gain matrix \mathbf{K} as $\{\mathbf{K}_i; \mathbf{K}_{-i}\}$.

In the multi-agent system (38), the single performance output \mathbf{z}_2 in (1) is replaced by N individual performance outputs of the agents $\mathbf{z}_{2,(i)}$. Assuming that each performance

output $\mathbf{z}_{2,(i)} = \mathbf{C}_{2,(i)}\mathbf{x} + \mathbf{D}_{2,(i)}\mathbf{u}_i$ has a form that satisfies (3), the H_2 -cost from \mathbf{w}_2 to agent i 's performance output can equivalently be defined as the individual LQR cost of agent i :

$$\begin{aligned} J_i(\mathbf{K}) &= \int_{t=0}^{\infty} [\mathbf{x}^T(t)\mathbf{Q}_i\mathbf{x}(t) + \mathbf{u}_i^T(t)\mathbf{R}_i\mathbf{u}_i(t)] dt \\ \text{s.t.} \quad & \mathbf{w}_1(t) = \mathbf{0}, \mathbf{w}_2(t) = \delta(t) \end{aligned} \quad (39)$$

where $\mathbf{Q}_i \in \mathbb{R}^{n \times n} \succeq 0$ and $\mathbf{R}_i \in \mathbb{R}^{q_i \times q_i} \succ 0$ are weight matrices for state and control input of agent i , respectively, and $\mathbf{w}_2(t)$ is an impulse disturbance. Similar to the centralized case, for stabilization of (37), the joint control strategy \mathbf{K} needs to satisfy (6).

In addition, we are interested in implementing a sparse controller subject to a global sparsity constraint. In the following, we develop a noncooperative game where agent i is modeled as a game player, with its strategy given by the control policy represented by \mathbf{K}_i . The joint strategies $\{\mathbf{K}_1, \mathbf{K}_2, \dots, \mathbf{K}_N\}$ must guarantee stability of the uncertain system (37) with at most s communication links in total. Thus, the set of admissible strategies $\{\mathbf{K}_1, \mathbf{K}_2, \dots, \mathbf{K}_N\}$ must satisfy

$$\|T_{z_1 w_1}(\{\mathbf{K}_1, \mathbf{K}_2, \dots, \mathbf{K}_N\})\|_\infty < \gamma, \quad (40)$$

$$\text{card}(\{\mathbf{K}_1, \mathbf{K}_2, \dots, \mathbf{K}_N\}) \leq s, \quad (41)$$

and the set of feasible strategies for player i , given other players' strategies \mathbf{K}_{-i} , must satisfy

$$\mathcal{G}_i(\mathbf{K}_{-i}) = \{\mathbf{K}_i | \text{card}(\{\mathbf{K}_i; \mathbf{K}_{-i}\}) \leq s,$$

$$\|T_{z_1 w_1}(\{\mathbf{K}_i; \mathbf{K}_{-i}\})\|_\infty < \gamma. \quad (42)$$

Given \mathbf{K}_{-i} , player i solves the following optimization:

$$\begin{aligned} \min_{\mathbf{K}_i} \quad & J_i(\{\mathbf{K}_i; \mathbf{K}_{-i}\}) \\ \text{s.t.} \quad & \mathbf{K}_i \in \mathcal{G}_i(\mathbf{K}_{-i}). \end{aligned} \quad (43)$$

Following [27], we can say that the set of strategies $(\mathbf{K}_1^*, \mathbf{K}_2^*, \dots, \mathbf{K}_N^*)$ is a Generalized Nash Equilibrium (GNE) if

$$J_i(\{\mathbf{K}_i^*; \mathbf{K}_{-i}^*\}) \leq J_i(\{\mathbf{K}_i; \mathbf{K}_{-i}^*\}), \quad \forall \mathbf{K}_i \in \mathcal{G}_i(\mathbf{K}_{-i}^*), \quad i = 1, \dots, N. \quad (44)$$

In GNE, no user can unilaterally deviate from the equilibrium to improve his utility given that the strategy satisfies the global constraint [27]. A GNE differs from Nash equilibrium (NE) due to the presence of global constraints.

B. PALM algorithm for GNE

We propose to solve the generalized Nash strategies (44) using the best-response dynamic (43) where each player takes its turn to maximize its payoff based on other players' strategies. The steps are listed in Algorithm 3. Recall Algorithm 1, where the tuple \mathbf{K}, \mathbf{F} was iteratively optimized to solve the penalized optimization (18). Similarly, given \mathbf{K}_{-i} , player i 's optimization (43) can be written in the penalized form using indicator functions as

$$\min_{\mathbf{K}_i, \mathbf{F}} \Phi_i(\mathbf{K}_i, \mathbf{F}; \mathbf{K}_{-i}) \quad (45)$$

with

$$\begin{aligned} \Phi_i(\mathbf{K}_i, \mathbf{F}; \mathbf{K}_{-i}) &\triangleq J_i(\{\mathbf{K}_i; \mathbf{K}_{-i}\}) + h(\{\mathbf{K}_i; \mathbf{K}_{-i}\}) \\ &\quad + f(\mathbf{F}) + H(\{\mathbf{K}_i; \mathbf{K}_{-i}\}, \mathbf{F}), \end{aligned} \quad (46)$$

where the indicator functions $h(\cdot)$ and $f(\cdot)$ are given by (16,17), and the matrix $\{\mathbf{K}_i; \mathbf{K}_{-i}\}$ is defined after (38). In

this optimization, $\mathbf{K}_i \in \mathbb{R}^{q_i \times n}$ is viewed as the feedback gain of agent i that satisfies $\|T_{z_1 w_1}(\{\mathbf{K}_i; \mathbf{K}_{-i}\})\|_\infty < \gamma$, and $\mathbf{F} \in \mathbb{R}^{m \times n}$ represents the system-wide sparse feedback gain matrix that satisfies the global sparsity constraint. In the function $\Phi(\mathbf{K}, \mathbf{F})$ (18), the variables \mathbf{K} and \mathbf{F} were of the same size, and they represented the same global sparsity-constrained feedback gain. However, when minimizing $\Phi_i(\mathbf{K}_i, \mathbf{F}; \mathbf{K}_{-i})$ (45), the variable \mathbf{K}_i is the robust feedback gain for player i while \mathbf{F} represents the global feedback gain that satisfies the sparsity constraint. In the best-response dynamic, in each round the players take turns to minimize their own respective Φ_i functions over \mathbf{K}_i and \mathbf{F} . The equilibrium point is achieved when no player can improve its Φ_i using \mathbf{K}_i and \mathbf{F} while \mathbf{K}_j is fixed for $j \neq i$. Note that in the initial best response update steps, given non-sparse \mathbf{K}_{-i} , the minimization objective (45) cannot drive the coupling function $H(\{\mathbf{K}_i; \mathbf{K}_{-i}\}, \mathbf{F})$ in (20) to zero. This is because $\sum_{i \neq j} \|\mathbf{K}_i - (\mathbf{F})_i\|_F^2 \approx 0$ only when \mathbf{K}_{-i} approaches the desired level of sparsity, where $(\mathbf{F})_i \in \mathbb{R}^{q_i \times n}$ denotes the row block of \mathbf{F} that corresponds to the feedback gain of the i^{th} player.

The minimization of (45) is similar to the minimization of (18). Thus, modified Algorithm 1 is used in line 9 of Algorithm 3 to solve (45). Given its \mathbf{K}_i^l , \mathbf{F}^l at iteration l , the following proximal operators are performed by player i in the minimization of line 9 of Algorithm 3.

1) **F-minimization** :

Compute the proximal point \mathbf{Z}^k for \mathbf{F}^k :

$$\begin{aligned} \mathbf{Z}^k &= \mathbf{F}^k - \frac{1}{a} \nabla_{\mathbf{F}} H(\mathbf{K}^k, \mathbf{F}^k) \\ &= \mathbf{F}^k - \frac{\gamma}{a} (\mathbf{F}^k - \{\mathbf{K}_i^k; \mathbf{K}_{-i}\}) \end{aligned} \quad (47)$$

Solve the proximal operator:

$$\begin{aligned} \mathbf{F}^{k+1} &= \arg \min_{\mathbf{F}} \frac{a}{2} \|\mathbf{F} - \mathbf{Z}^k\|_F^2 \\ &\text{s.t. } \text{card}(\mathbf{F}) \leq s, \end{aligned} \quad (48)$$

and get $\mathbf{F}^{k+1} = [\mathbf{Z}^k]_s$, similar to Step 2 of Algorithm 1.

2) **K-minimization** :

Algorithm 3 PALM algorithm for computing GNE (44)

- 1: **Given** s : global sparsity constraint, γ : H_∞ -norm bound.
 - 2: **Initialization**:
 - 3: \mathbf{K}^0 : any stabilizing feedback gain with $T_\infty(\mathbf{K}^0) < \gamma$.
 - 4: \mathbf{F}^0 : any stabilizing feedback gain \mathbf{F}^0 .
 - 5: **for** $l = 1 \dots l_{\max}$ until $\|\mathbf{F}^l - \mathbf{F}^{l-1}\|_F < \epsilon_3$ **do**
 - 6: $\mathbf{K}^l := \mathbf{K}^{l-1}$, $\mathbf{F}^l := \mathbf{F}^{l-1}$
 - 7: **for** $i = 1 \dots N$ **do**
 - 8: // Solve using (47–50) with \mathbf{K}_i^l , \mathbf{F}^l as the initial values:
 - 9: $\hat{\mathbf{K}}_i, \hat{\mathbf{F}} = \arg \min_{\mathbf{K}_i, \mathbf{F}} \Phi_i(\mathbf{K}_i, \mathbf{F}; \mathbf{K}_{-i}^l)$
 - 10: // Update \mathbf{K}^l and \mathbf{F}^l :
 - 11: $\mathbf{K}^l = \{\hat{\mathbf{K}}_i; \mathbf{K}_{-i}^l\}$
 - 12: $\mathbf{F}^l = \hat{\mathbf{F}}$
 - 13: **end for**
 - 14: **end for**
 - 15: **Output**: $\mathbf{K}^{\text{GNE}(s)} := \mathbf{F}^l$.
-

Compute proximal point \mathbf{X}_i^k for \mathbf{K}_i :

$$\begin{aligned} \mathbf{X}_i^k &= \mathbf{K}_i^k - \frac{1}{b} \nabla_{\mathbf{K}_i} H(\mathbf{K}_i^k - (\mathbf{F}^{k+1})_i) \\ &= \mathbf{K}_i^k - \frac{\rho}{b} (\mathbf{K}_i^k - (\mathbf{F}^{k+1})_i). \end{aligned} \quad (49)$$

Solve the proximal operator:

$$\begin{aligned} \mathbf{K}_i^{k+1} &= \arg \min_{\mathbf{K}_i} \left\{ J_i(\{\mathbf{K}_i; \mathbf{K}_{-i}\}) + \frac{b}{2} \|\mathbf{K}_i - \mathbf{X}_i^k\|_F^2 \right\} \\ &\text{s.t. } \|T_{z_1 w_1}(\{\mathbf{K}_i; \mathbf{K}_{-i}\})\|_\infty < \gamma. \end{aligned} \quad (50)$$

Solving (50) is similar to solving (31). In (50), player i aims to update its control strategy \mathbf{K}_i given other players' strategies \mathbf{K}_{-i} . Algorithm 2 is applied to solve (50) with several modifications. The minimization cost in (50) is defined as $h_i(\mathbf{K}_i, \mathbf{K}_{-i}) \triangleq J_i(\{\mathbf{K}_i; \mathbf{K}_{-i}\}) + \frac{b}{2} \|\mathbf{K}_i - \mathbf{X}_i^k\|_F^2$, and the gradient with respect to \mathbf{K}_i in line 4 of Algorithm 2 is replaced by

$$\nabla_{\mathbf{K}_i} h_i(\mathbf{K}_i, \mathbf{K}_{-i}) = \quad (51)$$

$2(\mathbf{R}_i \mathbf{K}_i \mathbf{C} - \mathbf{B}_{(i)}^T \mathbf{P}(\mathbf{K}_i, \mathbf{K}_{-i})) \mathbf{L}(\mathbf{K}_i, \mathbf{K}_{-i}) \mathbf{C}^T + b(\mathbf{K}_i - \mathbf{X}_i^k)$ where $L(\mathbf{K}_i, \mathbf{K}_{-i})$ and $P(\mathbf{K}_i, \mathbf{K}_{-i})$ are the solution of the following set of equations:

$$\begin{aligned} &(\bar{\mathbf{A}}_{cl}(\mathbf{K}_i, \mathbf{K}_{-i}))^T \mathbf{P}(\mathbf{K}_i, \mathbf{K}_{-i}) + \mathbf{P}(\mathbf{K}_i, \mathbf{K}_{-i}) \bar{\mathbf{A}}_{cl}(\mathbf{K}_i, \mathbf{K}_{-i}) \\ &+ \bar{\mathbf{Q}}_i(\mathbf{K}_i, \mathbf{K}_{-i}) = 0 \\ &\bar{\mathbf{A}}_{cl}(\mathbf{K}_i, \mathbf{K}_{-i}) \mathbf{L}(\mathbf{K}_i, \mathbf{K}_{-i}) + \mathbf{L}(\mathbf{K}_i, \mathbf{K}_{-i}) (\bar{\mathbf{A}}_{cl}(\mathbf{K}_i, \mathbf{K}_{-i}))^T \\ &+ \mathbf{B}_2 \mathbf{B}_2^T = 0 \end{aligned} \quad (52)$$

and

$$\bar{\mathbf{A}}_{cl}(\mathbf{K}_i, \mathbf{K}_{-i}) = \mathbf{A} - \sum_{j \neq i} \mathbf{B}_{(j)} \mathbf{K}_j \mathbf{C} - \mathbf{B}_{(i)} \mathbf{K}_i \mathbf{C} \quad (53)$$

$$\bar{\mathbf{Q}}_i(\mathbf{K}_i, \mathbf{K}_{-i}) = \mathbf{Q}_i + \mathbf{C}^T \left(\sum_{j \neq i} (\mathbf{K}_j)^T \mathbf{R}_j \mathbf{K}_j + \mathbf{K}_i^T \mathbf{R}_i \mathbf{K}_i \right) \mathbf{C}.$$

\mathbf{Q}_i and \mathbf{R}_i are defined in (39). Similar to lines 10–14 in Algorithm 2, when player i 's strategy $\mathbf{K}_i^{\text{cur}}$ is near the boundary of the H_∞ -norm constraint given other players' strategies \mathbf{K}_{-i} , an improving feasible direction for \mathbf{K}_i can be found by solving an LMI such as (36) for scalar z and $\mathbf{K}_i^{\text{in}} \in \mathbb{R}^{q_i \times n}$:

Maximize z
 $z, \mathbf{K}_i^{\text{in}}$

$$\text{s.t. } \text{trace}[(\nabla_{\mathbf{K}_i} h_i(\mathbf{K}_i^{\text{cur}}, \mathbf{K}_{-i}))^T (\mathbf{K}_i^{\text{in}} - \mathbf{K}_i^{\text{cur}})] + z \leq 0$$

$$\mathbf{G}(\{\mathbf{K}_i^{\text{in}}; \mathbf{K}_{-i}\}; \{\mathbf{K}_i^{\text{cur}}; \mathbf{K}_{-i}\}) - \theta z \cdot \mathbf{I} \succeq 0. \quad (54)$$

Here, θ is the factor to control the speed of reduction of H_∞ norm, and G is defined as in (34). Then the update direction of \mathbf{K}_i can be formed as $\Delta \mathbf{K}_i = \mathbf{K}_i^{\text{in}} - \mathbf{K}_i^{\text{cur}}$. We note that in \mathbf{K} -minimization step, each player updates its own strategy \mathbf{K}_i , while in \mathbf{F} -minimization step, the strategies of all the players are jointly updated. Thus, Algorithm 3 has partially distributed computation.

Finally, we note that the centralized problem (14) can be represented as a potential game by modifying the noncooperative game (44). A game $\{N, \{\mathcal{A}_i\}, \{J_i\}\}$ with N players, action set $\{\mathcal{A}_i\}_{i=1}^N$ and utilities $\{J_i\}_{i=1}^N$, is an exact potential game [35] if there exists a global function Φ , such that for every player $i \in N$, $a_{-i} \in \mathcal{A}_{-i}$ and $a'_i, a''_i \in \mathcal{A}_i$,

$$J_i(a'_i, a_{-i}) - J_i(a''_i, a_{-i}) = \Phi(a'_i, a_{-i}) - \Phi(a''_i, a_{-i}). \quad (55)$$

We employ a common assumption that the input penalty of each user is uncorrelated, i.e., $\mathbf{u}^T \mathbf{R} \mathbf{u} = \sum_{i=1}^N \mathbf{u}_i^T \mathbf{R}_{(i)} \mathbf{u}_i$, where $\mathbf{R}_{(i)}$ is the submatrix of \mathbf{R} that represents the weight

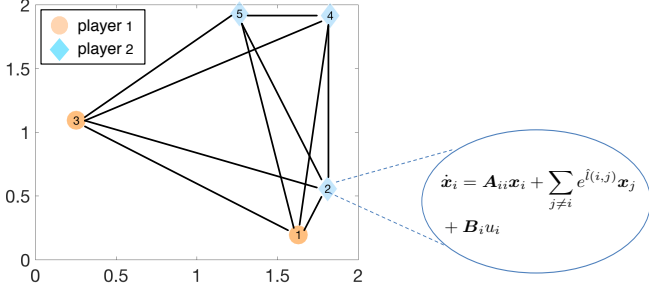


Fig. 1: The 5-node open-loop unstable network

matrix for $\mathbf{u}_i(t)$. Thus, the objective $J(\mathbf{K})$ in (13) can be expressed as

$$J(\mathbf{K}) = J(\{\mathbf{K}_i, \mathbf{K}_{-i}\}) = \int_0^\infty \left[\mathbf{x}^T \left(\mathbf{Q} + \mathbf{C}^T \left(\sum_{j \neq i} \mathbf{K}_j^T \mathbf{R}_{(j)} \mathbf{K}_j \right) \mathbf{C} \right) \mathbf{x} + \mathbf{u}_i^T \mathbf{R}_{(i)} \mathbf{u}_i \right] dt, \quad (56)$$

with $\mathbf{u}_i = -\mathbf{K}_i \mathbf{y}$. Thus, the minimization objectives $J_i(\{\mathbf{K}_i; \mathbf{K}_{-i}\})$ of all players in (43) are replaced by the global LQR cost (56). To convert the game in (43) into an exact potential game, we set $\mathbf{Q}_i = \mathbf{Q} + \mathbf{C}^T (\sum_{j \neq i} \mathbf{K}_j^T \mathbf{R}_{(j)} \mathbf{K}_j) \mathbf{C}$, $\mathbf{R}_i = \mathbf{R}_{(i)}$ in the individual cost (39), which is consistent with (56). The GNE strategies $\mathbf{K}_1^*, \mathbf{K}_2^*, \dots, \mathbf{K}_N^*$ for the potential game can be written as

$$\begin{aligned} J(\{\mathbf{K}_i^*; \mathbf{K}_{-i}^*\}) &\leq J(\{\mathbf{K}_i; \mathbf{K}_{-i}^*\}), \\ \forall \mathbf{K}_i &\in \mathcal{G}_i(\mathbf{K}_{-i}^*), \quad i = 1, \dots, N. \end{aligned} \quad (57)$$

We employ Algorithm 3 to compute (57). Players update their control strategies in the \mathbf{K} -minimization step distributively, and jointly update their strategies in the \mathbf{F} -minimization step, thereby obtaining a partially distributed implementation of the centralized sparsity-constrained problem (14).

IV. NUMERICAL RESULTS AND CONVERGENCE ANALYSIS

A. Network model

We consider an example of an uncertain network model from [36]. The network consists of N connected nodes distributed randomly on a L unit by L unit square area. Each node is an unstable second-order system coupled with other nodes through an exponentially decaying function of the Euclidean distance $\hat{l}(i, j)$ [1], [36]. The state-space representation of node i is given as:

$$\begin{bmatrix} \dot{x}_{1i} \\ \dot{x}_{2i} \end{bmatrix} = \hat{\mathbf{A}}_{ii} \begin{bmatrix} x_{1i} \\ x_{2i} \end{bmatrix} + \sum_{j \neq i} e^{-\hat{l}(i,j)} \begin{bmatrix} x_{1j} \\ x_{2j} \end{bmatrix} + \begin{bmatrix} 0 \\ 1 \end{bmatrix} (d_i + u_i). \quad (58)$$

In the above state-space representation, the state matrix $\hat{\mathbf{A}}_{ii}$, $i = 1, \dots, N$ and the Euclidean distances $\hat{l}(i, j)$ are not known exactly. In particular,

$$\begin{aligned} \hat{\mathbf{A}}_{ii} &= \mathbf{A}_{ii} + \mathbf{A}_{ii} \odot \begin{bmatrix} \theta_{11} & \theta_{12} \\ \theta_{21} & \theta_{22} \end{bmatrix} \\ \hat{l}(i, j) &= l(i, j) \cdot (1 + \delta_{i,j}), \end{aligned} \quad (59)$$

where \mathbf{A}_{ii} and $l(i, j)$ are the nominal values, and δ_{ij} and θ_{ij} are independent random perturbations, uniformly distributed in the range $\pm 20\%$. The operator \odot denotes element-wise multiplication. As in (1), \mathbf{A} denotes the nominal value of the state matrix of this N -node unstable system, and $\hat{\mathbf{A}}$

denotes one realization of the perturbed state matrix. The uncertain matrix $\Delta \mathbf{A} = \hat{\mathbf{A}} - \mathbf{A}$ in (1). The control input matrix is assumed to be known for this example, so that $\hat{\mathbf{B}} = \mathbf{B} = \mathbf{1}_N \otimes \mathbf{B}_{ii}$, where $\mathbf{B}_{ii} = \begin{bmatrix} 0 & 1 \end{bmatrix}^T$, and \otimes denotes the Kronecker product [37]. In this simulation study, we collected 200 random samples of $\hat{\mathbf{A}}$. To guarantee closed-loop stability of (58), we numerically compute the worst-case $\hat{\mathbf{A}}$ as,

$$\hat{\mathbf{A}}_{\text{worst}} = \arg \max_{\hat{\mathbf{A}}} \sigma_{\max}(\hat{\mathbf{A}} - \mathbf{A}). \quad (60)$$

Using the singular value decomposition, we obtain $USV^T = \hat{\mathbf{A}}_{\text{worst}} - \mathbf{A}$. Normalizing \mathbf{S} by $\sigma_{\max}(\mathbf{S})$, we set $\mathbf{B}_1 = \sqrt{\sigma_{\max}(\mathbf{S})} \mathbf{U}$, $\mathbf{C}_1 = \sqrt{\sigma_{\max}(\mathbf{S})} \mathbf{V}^T$ in (2). Due to this normalization, $\gamma = 1$.

The following parameters are employed in the simulations. We set $L = 2$ and $N = 5$, thus $\mathbf{A} \in \mathbb{R}^{10 \times 10}$, $\mathbf{B} \in \mathbb{R}^{10 \times 5}$. The output matrix $\mathbf{C} = \mathbf{I}_{10}$. The dense feedback matrix \mathbf{K} has $\text{card}(\mathbf{K}) = 50$. When the feedback controller is completely decentralized, i.e., feedback links only exist between states and controllers within the same node, $\text{card}(\mathbf{K}) = 10$. The performance index for the LQR cost employs $\mathbf{Q} = 100 \cdot \mathbf{I}$ and $\mathbf{R} = \mathbf{I}$ in (12) for the centralized problem (14). For the noncooperative game (44), we consider a two-player game as shown in Figure 1, where player 1 is in charge of the control inputs in nodes 1 and 3 and player 2 is in charge of the control inputs in nodes 2, 4, 5. The performance index matrices $\mathbf{Q}_i, \mathbf{R}_i$, $i = 1, 2$ for the LQR cost in (39) satisfy:

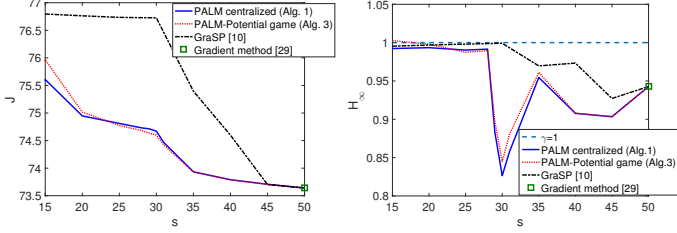
$$\begin{aligned} \mathbf{x}^T \mathbf{Q}_1 \mathbf{x} + \mathbf{u}_1^T \mathbf{R}_1 \mathbf{u}_1 &= 100[(x_{11} - x_{13})^2 + (x_{21} - x_{23})^2] + u_1^2 + u_3^2 \\ \mathbf{x}^T \mathbf{Q}_2 \mathbf{x} + \mathbf{u}_2^T \mathbf{R}_2 \mathbf{u}_2 &= 100 \sum_{j=2,4,5} (x_{1j}^2 + x_{2j}^2) + \sum_{j=2,4,5} u_j^2. \end{aligned} \quad (61)$$

We solve all the LMIs using the CVX package [38].

B. Social optimization

First, we present simulation results for the problem (14) applied to the system in (58) with $\gamma = 1$ in (14) over a range of s -values. We implement Algorithm 1, with the resulting feedback matrix denoted as $\mathbf{K}_{\text{palm}}^*(s)$. For the same problem (14), we also use Algorithm 3 applied to the potential game (57), with the solution denoted by $\mathbf{K}_{\text{PALMPG}}^*(s)$, given the sparsity constraint s . For comparison, we also run the GraSP algorithm that was used in [24], with the resulting feedback denoted by $\mathbf{K}_{\text{GraSP}}^*(s)$, initialized by a stabilizing decentralized controller \mathbf{K}_{dec} with $\text{card}(\mathbf{K}_{\text{dec}}) = 10$. In general, GraSP needs to be initialized by a \mathbf{K}_0 that satisfies $\text{card}(\mathbf{K}_0) \leq s$ and $T_\infty(\mathbf{K}_0) < \gamma$, which in reality might be difficult to find. In contrast, the PALM-based Algorithm 1 of this paper does not rely on any such sparse initialization. Finally, we show performance of the dense mixed H_2/H_∞ controller using the simple gradient method in [28].

Figure 2 illustrates the optimal LQR cost J in problem (14) and the associated H_∞ norm vs. sparsity constraint s . For $15 \leq s \leq 50$, the centralized Algorithm 1 and the potential game using Algorithm 3 both converge to a solution with sufficiently small coupling function in (18), which indicates $\mathbf{F} \approx \mathbf{K}$. From Figure 2(a), we observe that the H_2 norms of all sparsity-constrained methods decrease as s is relaxed, and approach to that of the dense controller [4]. However, the



(a) J vs. sparsity constraint s . (b) H_∞ norm v.s. sparsity constraint s .
Fig. 2: The LQR cost J and H_∞ norm vs. sparsity constraint s .

PALM-based methods have similar LQR costs and outperform significantly the greedy GraSP algorithm in [24]. In GraSP, the choice of active coordinates only depends on the gradient information of the function J . At convergence, the solution of the mixed H_2/H_∞ problem has the sparsity structure given by the greedy selection step. For the PALM algorithm, since we iteratively compute the proximal map on \mathbf{X}^k and \mathbf{Z}^k , the support is chosen based on the information on both the LQR cost $J(\mathbf{K})$ and the H_∞ -norm constraint $T_\infty(\mathbf{K})$. Thus, at convergence, the PALM method finds a critical point of problem (14) while GraSP does not necessarily achieve it. Figure 2(b) shows the H_∞ norms of $\mathbf{K}_{\text{PALM}}^*(s)$, $\mathbf{K}_{\text{PALMPG}}^*(s)$ and $\mathbf{K}_{\text{GraSP}}^*(s)$. We observe that for both GraSP and PALM methods, the solution is found in the interior of the H_∞ -norm constraint for $s \geq 30$, and on the boundary for $s \leq 25$, which indicates that when the sparsity constraint becomes more stringent, satisfying the sparsity and H_∞ -norm constraints simultaneously becomes challenging.

Both Algorithm 1 (the social optimization) and Algorithm 3 (the potential game) are found to converge for all s -values for this system. Figure 3 shows the error in consecutive steps for variable \mathbf{K} at the end of step 3 of Algorithm 1 as a function of iteration step, for different s -values. We found that $\Delta \mathbf{F}_k$ has a similar trend to $\Delta \mathbf{K}_k$. The errors in consecutive steps are defined as $\Delta \mathbf{K}^k \triangleq \mathbf{K}^k - \mathbf{K}^{k-1}$ and $\Delta \mathbf{F}^k \triangleq \mathbf{F}^k - \mathbf{F}^{k-1}$. We note that the error converges faster for larger s -values, which might be explained by the fact that for $s > 25$, the minima are found in the interior of the H_∞ -norm constraint set (see Figure 2). For Algorithm 3 (potential game), the penalized cost function Φ_i and $\|\mathbf{K} - \mathbf{F}\|_F^2$ (line 9) have similar trends to those for Algorithm 1. Moreover, it is demonstrated in Fig 4 that although Algorithm 1 converges to a critical point of $\Phi(\mathbf{K}, \mathbf{F})$, the coupling function $H(\mathbf{K}, \mathbf{F}) > 0$ for $s < 15$. As a result, when Algorithm 1 converges for these s -values, $\mathbf{K} \neq \mathbf{F}$, so a sparse feedback solution that satisfies (14) cannot be found. Thus, in Figure 2, we only show the LQR cost and H_∞ -norm for $15 \leq s \leq 50$.

C. The noncooperative game

We investigate performance of Algorithm 3 for the noncooperative game with different individual costs (61) for the system (58). We use $\mathbf{K}^{\text{GNE}}(s) = \{\mathbf{K}_1^{\text{GNE}}(s), \mathbf{K}_2^{\text{GNE}}(s)\}$ to denote the two players' feedback produced by Algorithm 3 when the sparsity constraint is given by s . Figure 5 shows the errors in consecutive steps of player i 's strategic variables $\mathbf{K}_i, \mathbf{F}_i$ for $i = 1, 2$ vs iteration round l in Algorithm 3. We observe that

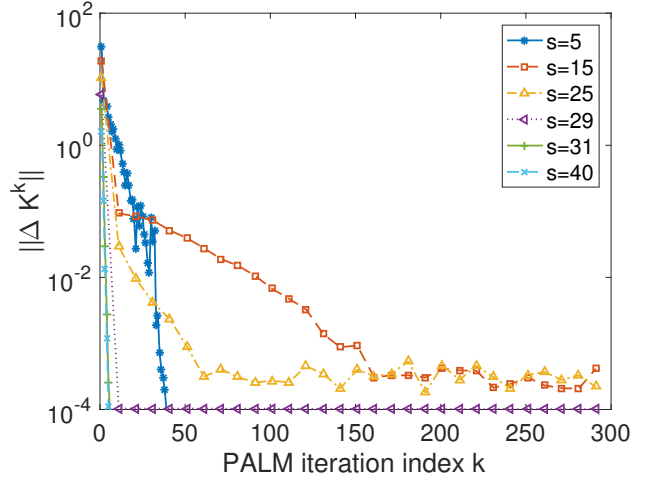


Fig. 3: The error in \mathbf{K} vs. iteration k in PALM Algorithm 1 Step 2 and 3 for different s -values.

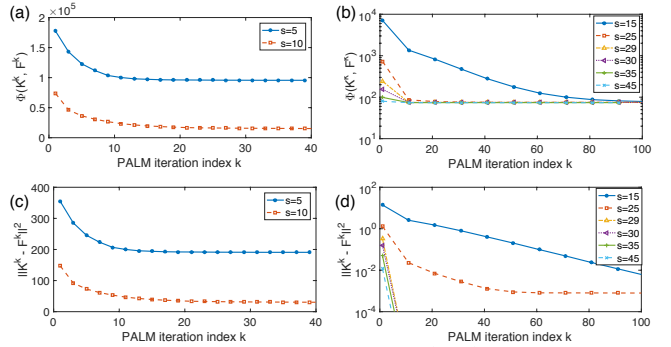


Fig. 4: The penalized cost function $\Phi(\mathbf{K}^k, \mathbf{F}^k)$ and the coupling function $\|\mathbf{K}^k - \mathbf{F}^k\|_F^2$ vs iteration k in the end of Step 3 of Algorithm 1 for multiple s -values.

both $\|\Delta \mathbf{K}_i\|_F$ and $\|\Delta \mathbf{F}_i\|_F$ decrease significantly within the first 10 iterations and then saturate to small values as l grows, resulting in the saturation of the penalized cost function Φ_i in line 9 of Algorithm 3, which corresponds to an approximate equilibrium point as discussed in section IV-D. The normalized coupling function $\frac{1}{\rho} H(\mathbf{K}^l, \mathbf{F}^l) = \|\mathbf{K}^l - \mathbf{F}^l\|_F^2$ (20) decreases with iteration l , following the trend in Figure 4. For $s > 20$, the square error $\|\mathbf{K}^l - \mathbf{F}^l\|_F^2$ reaches a sufficiently small value ($< 10^{-4}$) at the equilibrium point, while for $s \leq 20$, the square error is larger, causing $T_\infty(\mathbf{K}^{\text{GNE}}(s)) > T_\infty(\mathbf{K}^l)$, which results in $T_\infty(\mathbf{K}^{\text{GNE}}(s)) > 1$ during convergence. One way to avoid this discrepancy and still guarantee closed-loop stability is to replace γ in (16) with $\gamma - \epsilon$, and provide a margin that compensates for the square error between \mathbf{K} and \mathbf{F} . For this example, we set $\epsilon = 0.01$, so that $T_\infty(\mathbf{K}^{\text{GNE}}(s)) < 0.99$.

Figure 6 illustrates the individual LQR costs J_i as in (39), and the global H_∞ norm when $\mathbf{K}^{\text{GNE}}(s)$ is implemented. We observe that in Figure 6(a), for each player i , the LQR cost achieved at the equilibrium point $J_i(\mathbf{K}^{\text{GNE}}(s))$ tends to decrease with s , which indicates that there is a trade-off between the selfish LQR cost and the global shared sparsity constraint. Figure 6(b) shows that $T_\infty(\mathbf{K}^{\text{GNE}}(s)) < 1$ for $15 \leq s \leq 45$, indicating that the Nash strategies in $\mathbf{K}^{\text{GNE}}(s)$ are guaranteed to stabilize the uncertain system (58).

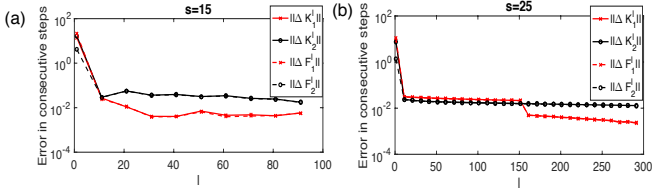
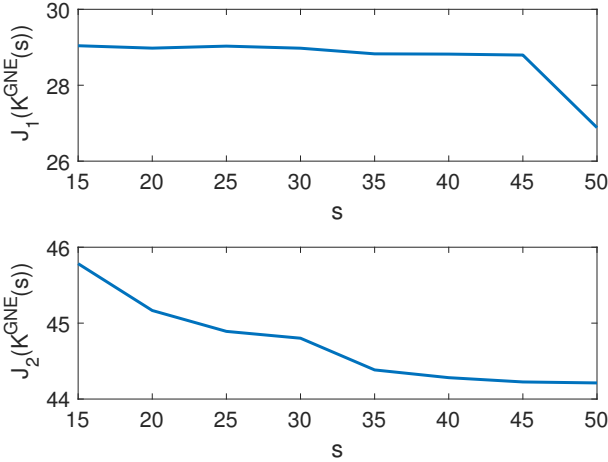
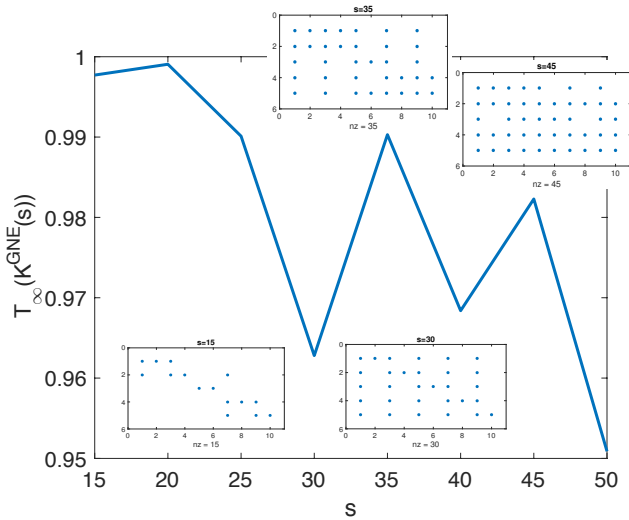


Fig. 5: Errors in consecutive steps of \mathbf{K}_i^l and \mathbf{F}_i^l for players $i = 1, 2$ vs. step l in Algorithm 3 (the noncooperative game).



(a) $J_i(\mathbf{K}^{\text{GNE}}(s))$ vs. sparsity constraint s at GNE for $i = 1, 2$.



(b) $T_\infty(\mathbf{K}^{\text{GNE}}(s))$ vs. the sparsity constraint s at GNE.

Fig. 6: The individual LQR cost and global H_∞ norm of $\mathbf{K}^{\text{GNE}}(s)$ vs sparsity constraint s at GNE and the sparsity pattern of $\mathbf{K}^{\text{GNE}}(s)$ for different s values.

D. Algorithm Convergence and Complexity

We close this section by providing some final comments about the convergence properties and complexity of the proposed algorithms. Global convergence of PALM for nonconvex nonsmooth functions was studied in [25], while that of PALM-based output feedback co-design under block-sparsity constraints was established in [5]. Results in [5], [25] are extended to analyze the convergence properties of Algorithm 1 in [30], [31]. It has been proven in [Bolte et al., 2014] that

if Lemma 2–4 in [30] hold, then the sequence generated by PALM algorithm globally converges. In addition, if Lemma 5 of [30] holds, the sequence converges to a critical point [Bolte et al., 2014] of Φ . This confirms convergence of Algorithm 1 to a sparsity-constrained mixed H_2/H_∞ controller, which corresponds to a critical point of Φ under mild assumptions on the functions J and g .

Next, we briefly discuss the convergence properties of Algorithm 3. Suppose a GNE (44) is given by $(\mathbf{K}_1^*, \dots, \mathbf{K}_N^*)$. Then the following condition holds for each player i [39]:

$$\nabla_{\mathcal{G}_i(\mathbf{K}_{-i}^*), \eta} J_i(\{\mathbf{K}_i^*; \mathbf{K}_{-i}^*\}) = 0, \quad (62)$$

where $\nabla_{\mathcal{G}_i(\mathbf{K}_{-i}^*), \eta} J_i(\{\mathbf{K}_i; \mathbf{K}_{-i}^*\})$ is the projected gradient of cost J_i (39) onto the constraint set \mathcal{G}_i (42) for player i , $i = 1, \dots, N$. Again, from [39], we can write

$$\nabla_{\mathcal{G}_i(\mathbf{K}_{-i}^*), \eta} J_i(\{\mathbf{K}_i; \mathbf{K}_{-i}^*\}) \triangleq \frac{1}{\eta} (\mathbf{K}_i - \Pi_{\mathcal{G}_i(\mathbf{K}_{-i}^*)} [\mathbf{K}_i - \eta \nabla_{\mathbf{K}_i} J_i(\{\mathbf{K}_i, \mathbf{K}_{-i}^*\})]) \quad (63)$$

where $\eta > 0$ and the operator $\Pi_{\mathcal{K}}(\cdot)$ denotes projection onto the set \mathcal{K} .

Similarly, in line 9 of Algorithm 3, a necessary condition for Φ_i to achieve its minimum is that the projected gradient $\nabla_{\mathcal{G}_i(\mathbf{K}_{-i}^*), \eta} J_i(\{\mathbf{K}_i; \mathbf{K}_{-i}^*\}) = 0$. Instead of seeking an exact equilibrium point as GNE, we assume convergence of Algorithm 3 when this projected gradient is sufficiently small, which is a necessary condition for an approximate local equilibrium [39]. At iteration l , the $\hat{\mathbf{K}}_i$ in line 9 can be viewed as an approximation of $\Pi_{\mathcal{G}_i(\mathbf{K}_{-i}^*)} [\mathbf{K}_i^{l-1} - \eta \nabla_{\mathbf{K}_i} J_i(\{\mathbf{K}_i^{l-1}, \mathbf{K}_{-i}^*\})]$. Thus, the norm of the projected gradient is proportional to $\|\mathbf{K}_i^l - \mathbf{K}_i^{l-1}\|$, implying that small values of $\Delta \mathbf{K}_i^l$ and $\Delta \mathbf{F}_i^l$ indicate convergence of Algorithm 3. This is illustrated in Figure 5. Moreover, we note that there is no theoretical guarantee for the existence of GNE for the game in (43). If a GNE exists for the potential game (57) then this GNE satisfies the necessary condition for the minimizer of (14).

The main numerical complexity of Algorithms 1 and 3 is dominated by the \mathbf{K} -minimization step (Step 3 of Algorithm 1 and line 9 of Algorithm 3), which has polynomial complexity on the number of variables in the feedback matrix [40].

V. CONCLUSION

The PALM method was exploited to solve the sparsity-constrained mixed H_2/H_∞ control problem for multi-agent systems. First, a centralized social-optimization algorithm was investigated. Second, we developed noncooperative and potential games that have partially-distributed computation. The proposed algorithms were validated using an open-loop unstable network dynamic system. It was demonstrated that the centralized PALM method outperforms the GraSP-based method for most sparsity levels, and converges both theoretically as well as in simulation results. Moreover, a best-response dynamics algorithm for the proposed games converges to an approximate GNE point. The performance of the potential game for social optimization closely approximates that of the centralized algorithm.

REFERENCES

- [1] F. Lin, M. Fardad, and M. R. Jovanović, “Design of optimal sparse feedback gains via the alternating direction method of multipliers,” *IEEE Trans. on Aut. Ctrl.*, vol. 58, no. 9, pp. 2426–2431, 2013.
- [2] F. Lian, A. Chakraborty, and A. Duel-Hallen, “Game-theoretic multi-agent control and network cost allocation under communication constraints,” *IEEE Journal on Selected Areas in Communications*, vol. 35, no. 2, pp. 330–340, 2017.
- [3] N. Monshizadeh, H. L. Trentelman, and M. K. Camlibel, “Projection-based model reduction of multi-agent systems using graph partitions,” *IEEE Trans. on Control of Network Systems*, vol. 1, no. 2, pp. 145–154, 2014.
- [4] F. Dörfler, M. R. Jovanović, M. Chertkov, and F. Bullo, “Sparsity-promoting optimal wide-area control of power networks,” *IEEE Trans. on Power Systems*, vol. 29, no. 5, pp. 2281–2291, 2014.
- [5] F. Lin and V. Adetola, “Co-design of sparse output feedback and row/column-sparse output matrix,” in *American Control Conference (ACC)*, 2017. IEEE, 2017, pp. 4359–4364.
- [6] N. Matni and V. Chandrasekaran, “Regularization for design,” *IEEE Transactions on Automatic Control*, vol. 61, no. 12, pp. 3991–4006, 2016.
- [7] C. Lidström and A. Rantzer, “Optimal H_∞ state feedback for systems with symmetric and hurwitz state matrix,” in *American Control Conference*, 2016, pp. 3366–3371.
- [8] R. Arastoo, M. Bahavarnia, M. V. Kothare, and N. Motee, “Closed-loop feedback sparsification under parametric uncertainties,” in *IEEE 55th Conference on Decision and Control*, 2016, pp. 123–128.
- [9] M. Bahavarnia and N. Motee, “Sparse memoryless LQR design for uncertain linear time-delay systems,” *IFAC-PapersOnLine*, vol. 50, no. 1, pp. 10395–10400, 2017.
- [10] M. Bahavarnia, C. Somarakis, and N. Motee, “State feedback controller sparsification via a notion of non-fragility,” in *Decision and Control (CDC), 2017 IEEE 56th Annual Conference on*. IEEE, 2017, pp. 4205–4210.
- [11] S. Seuken and S. Zilberstein, “Formal models and algorithms for decentralized decision making under uncertainty,” *Autonomous Agents and Multi-Agent Systems*, vol. 17, no. 2, pp. 190–250, 2008.
- [12] P. Ogren, E. Fiorelli, and N. E. Leonard, “Cooperative control of mobile sensor networks: Adaptive gradient climbing in a distributed environment,” *IEEE Transactions on Automatic control*, vol. 49, no. 8, pp. 1292–1302, 2004.
- [13] M. Jungers, E. B. Castelan, E. R. De Pieri, and H. Abou-Kandil, “Bounded nash type controls for uncertain linear systems,” *Automatica*, vol. 44, no. 7, pp. 1874–1879, 2008.
- [14] N. de la Cruz and M. Jimenez-Lizarraga, “Finite time robust feedback nash equilibrium for linear quadratic games,” *IFAC-PapersOnLine*, vol. 50, no. 1, pp. 11794–11799, 2017.
- [15] T. Başar and G. J. Olster, *Dynamic noncooperative game theory*. SIAM, 1995, vol. 200.
- [16] H. Mukaidani, “Robust guaranteed cost control for uncertain stochastic systems with multiple decision makers,” *Automatica*, vol. 45, no. 7, pp. 1758–1764, 2009.
- [17] —, “ H_2/H_∞ control problem for stochastic delay systems with multiple decision makers,” in *Decision and Control (CDC), 2014 IEEE 53rd Annual Conference on*. IEEE, 2014, pp. 2648–2653.
- [18] H. Mukaidani and H. Xu, “Stackelberg strategies for stochastic systems with multiple followers,” *Automatica*, vol. 53, pp. 53–59, 2015.
- [19] H. Mukaidani, H. Xu, and V. Dragan, “Dynamic games for markov jump stochastic delay systems,” in *Recent Results on Time-Delay Systems*. Springer, 2016, pp. 207–227.
- [20] D. Vrabie and F. Lewis, “Integral reinforcement learning for online computation of feedback nash strategies of nonzero-sum differential games,” in *Decision and Control (CDC), 2010 49th IEEE Conference on*. IEEE, 2010, pp. 3066–3071.
- [21] K. G. Vamvoudakis, “Non-zero sum Nash Q-learning for unknown deterministic continuous-time linear systems,” *Automatica*, vol. 61, pp. 274–281, 2015.
- [22] R. Song, F. L. Lewis, and Q. Wei, “Off-policy integral reinforcement learning method to solve nonlinear continuous-time multiplayer nonzero-sum games,” *IEEE transactions on neural networks and learning systems*, vol. 28, no. 3, pp. 704–713, 2017.
- [23] K. G. Vamvoudakis, H. Modares, B. Kiumarsi, and F. L. Lewis, “Game theory-based control system algorithms with real-time reinforcement learning: How to solve multiplayer games online,” *IEEE Control Systems*, vol. 37, no. 1, pp. 33–52, 2017.
- [24] F. Lian, A. Chakraborty, F. Wu, and A. Duel-Hallen, “Sparsity-constrained mixed H_2/H_∞ control,” in *American Control Conference (ACC)*, 2018, 2018.
- [25] J. Bolte, S. Sabach, and M. Teboulle, “Proximal alternating linearized minimization or nonconvex and nonsmooth problems,” *Mathematical Programming*, vol. 146, no. 1-2, pp. 459–494, 2014.
- [26] S. Bahmani, B. Raj, and P. T. Boufounos, “Greedy sparsity-constrained optimization,” *The Journal of Machine Learning Research*, vol. 14, no. 1, pp. 807–841, 2013.
- [27] D. Paccagnan, B. Gentile, F. Parise, M. Kamgarpour, and J. Lygeros, “Distributed computation of generalized nash equilibria in quadratic aggregative games with affine coupling constraints,” in *Decision and Control (CDC), 2016 IEEE 55th Conference on*. IEEE, 2016, pp. 6123–6128.
- [28] Y. Kami and E. Nobuyama, “A gradient method for the static output feedback mixed H_2/H_∞ control,” *IFAC Proceedings Volumes*, vol. 41, no. 2, pp. 7838–7842, 2008.
- [29] N. Parikh, S. Boyd *et al.*, “Proximal algorithms,” *Foundations and Trends® in Optimization*, vol. 1, no. 3, pp. 127–239, 2014.
- [30] F. Lian, A. Chakraborty, and A. Duel-Hallen, “Supplementary materials for ‘Game-theoretic mixed h_2/h_∞ control with sparsity constraint for multi-agent networked control systems’.”
- [31] F. Lian, “Communication-cost-constrained algorithms and games for multi-agent control systems,” Ph.D. dissertation, North Carolina State University, Raleigh, NC, USA, 2019.
- [32] D. G. Luenberger and Y. Ye, *Linear and nonlinear programming*. Springer, 1984, vol. 2.
- [33] M. S. Bazaraa, H. D. Sherali, and C. M. Shetty, *Nonlinear programming: theory and algorithms*. John Wiley & Sons, 2013.
- [34] M. Saeki, “Static output feedback design for H_∞ control by descent method,” in *45th IEEE Conference on Decision and Control*, 2006, pp. 5156–5161.
- [35] N. Li and J. R. Marden, “Designing games for distributed optimization,” *IEEE Journal of Selected Topics in Signal Processing*, vol. 7, no. 2, pp. 230–242, 2013.
- [36] N. Motee and A. Jadbabaie, “Optimal control of spatially distributed systems,” *IEEE Trans. on Aut. Ctrl.*, vol. 53, no. 7, pp. 1616–1629, 2008.
- [37] C. D. Meyer, *Matrix analysis and applied linear algebra*. Siam, 2000, vol. 71.
- [38] M. Grant and S. Boyd, “CVX: Matlab software for disciplined convex programming, version 2.1,” <http://cvxr.com/cvx>, Mar. 2014.
- [39] E. Hazan, K. Singh, and C. Zhang, “Efficient regret minimization in non-convex games,” *arXiv preprint arXiv:1708.00075*, 2017.
- [40] P. Gahinet, A. Nemirovskii, A. J. Laub, and M. Chilali, “The lmi control toolbox,” in *Proceedings of 1994 33rd IEEE Conference on Decision and Control*, vol. 3. IEEE, 1994, pp. 2038–2041.

Supplemental Materials for “Game-Theoretic Mixed H_2/H_∞ Control with Sparsity Constraint for Multi-agent Networked Control Systems” by Feier Lian, Aranya Chakraborty, and Alexandra Duel-Hallen

S.I: OVERVIEW OF ZOUTENDIJK’S METHOD

The Zoutendijk’s method [Bazaraa et al., 2013] is an approach to constrained optimization, where an improving feasible direction is generated by solving a subproblem, usually a linear program. We briefly overview Zoutendijk’s method for the case of nonlinear inequality constraints.

Consider the following constrained optimization problem:

$$\begin{aligned} \text{Minimize} \quad & f(\mathbf{x}) \\ \text{s.t.} \quad & g_i(\mathbf{x}) \leq 0, \quad i = 1, \dots, m, \end{aligned} \quad (\text{S1})$$

where $\mathbf{x} \in \mathbb{R}^{n \times 1}$ and $f(\mathbf{x})$ and $g_i(\mathbf{x})$ are differentiable at \mathbf{x} . At point \mathbf{x} , I is the set of active constraint $I = \{i | g_i(\mathbf{x}) = 0\}$. An improving feasible direction \mathbf{d} can be found by the following linear programming problem [Bazaraa et al., 2013]:

$$\begin{aligned} \text{Maximize} \quad & z \\ \text{s.t.} \quad & \nabla f(\mathbf{x})^T \mathbf{d} + z \leq 0, \\ & \nabla g_i(\mathbf{x})^T \mathbf{d} + z \leq 0 \quad \forall i \in I, \\ & -1 \leq d_j \leq 1, \quad \forall j = 1, \dots, n, \end{aligned} \quad (\text{S2})$$

where the third normalizing constraint prevents the optimal z from approaching ∞ . It was shown [Bazaraa et al., 2013] that if the optimal value of z , denoted as z^* , satisfies $z^* > 0$, then \mathbf{d} is an improving direction since \mathbf{d} satisfies $\nabla f(\mathbf{x})^T \mathbf{d} < 0$ and $\nabla g_i(\mathbf{x})^T \mathbf{d} < 0 \quad \forall i \in I$. Otherwise if $z^* = 0$, then the current \mathbf{x} is a Fritz John point [Bazaraa et al., 2013], which satisfies the necessary condition for the local minimum of (S1).

S.II: DEFINITIONS OF TERMS IN SECTION II-C

Definition 1. (Lipschitz constant) A function $f : \mathbb{R}^d \rightarrow \mathbb{R}$ with the gradient function ∇f is Lipschitz continuous with Lipschitz constant L on $\mathcal{S} \in \mathbb{R}^d$ if $\|\nabla f(\mathbf{x}) - \nabla f(\mathbf{y})\| \leq L\|\mathbf{x} - \mathbf{y}\|$ for all $\mathbf{x}, \mathbf{y} \in \mathcal{S}$ [Bazaraa et al., 2013].

Definition 2. (Proper) The function $\sigma : \mathcal{S} \rightarrow \mathbb{R}$ is a proper function if $\sigma(\mathbf{x}) > -\infty$ for all $\mathbf{x} \in \mathcal{S}$, and $\sigma(\mathbf{x}) < \infty$ for at least one point $\mathbf{x} \in \mathcal{S}$.

Definition 3. (Lower semicontinuous) The function $\sigma : \mathcal{S} \rightarrow \mathbb{R}$ is lower semicontinuous at $\bar{\mathbf{x}} \in \mathcal{S}$ if for all $\epsilon > 0$ there exists a δ such that $\mathbf{x} \in \mathcal{S}$ and $\|\mathbf{x} - \bar{\mathbf{x}}\| < \delta$ imply $\sigma(\mathbf{x}) - \sigma(\bar{\mathbf{x}}) > -\epsilon$.

S.III: NOTATION USED IN KURDYKA-ŁOJASIEWICZ (KL) PROPERTY, EMPLOYED IN CONVERGENCE ANALYSIS OF ALGORITHM 1

Definition 4. (Distance.) For any subset $\mathcal{S} \subset \mathbb{R}^d$ and any point $x \in \mathbb{R}^d$, the distance from x to \mathcal{S} is defined and denoted by

$$\text{dist}(\mathbf{x}, \mathcal{S}) := \inf\{\|\mathbf{y} - \mathbf{x}\| : \mathbf{y} \in \mathcal{S}\}. \quad (\text{S3})$$

When $\mathcal{S} = \emptyset$, we have $\text{dist}(\mathbf{x}, \mathcal{S}) = \infty$ for all \mathbf{x} .

Let $\eta \in [0, \infty]$. We denote by Φ_η the class of all concave and continuous functions $\varphi : [0, \eta] \rightarrow \mathbb{R}_+$ which satisfy the following conditions:

- (i) $\varphi(0) = 0$.
- (ii) φ has first-order continuous derivative on $(0, \eta)$ and continuous at 0;
- (iii) for all $s \in (0, \eta) : \varphi'(s) > 0$.

For proper and lower semicontinuous functions, the subdifferentials are defined below [Bolte et al., 2014]:

Definition 5. (Subdifferentials) Let $\sigma : \mathbb{R}^d \rightarrow (-\infty, \infty]$ be a proper and lower semicontinuous function.

(i) For a given $\mathbf{x} \in \text{dom } \sigma$, the Fréchet subdifferential of σ at x , written as $\hat{\partial}\sigma(\mathbf{x})$, is the set of all vectors $\mathbf{u} \in \mathbb{R}^d$ which satisfy

$$\liminf_{\mathbf{y} \neq \mathbf{x}, \mathbf{y} \rightarrow \mathbf{x}} \frac{\sigma(\mathbf{y}) - \sigma(\mathbf{x}) - \langle \mathbf{u}, \mathbf{y} - \mathbf{x} \rangle}{\|\mathbf{y} - \mathbf{x}\|} \geq 0. \quad (\text{S4})$$

When $\mathbf{x} \notin \text{dom } \sigma$, we set $\hat{\partial}\sigma(\mathbf{x}) = \emptyset$.

(ii) The limiting subdifferential, or subdifferential, of σ at $\mathbf{x} \in \mathbb{R}^d$, written as $\partial\sigma(\mathbf{x})$, is defined as

$$\begin{aligned} \partial\sigma(\mathbf{x}) \quad & := \left\{ \mathbf{u} \in \mathbb{R}^d : \exists \mathbf{x}^k \rightarrow \mathbf{x}, \sigma(\mathbf{x}^k) \rightarrow \sigma(\mathbf{x}) \right. \\ & \left. \text{and } \mathbf{u}^k \in \hat{\partial}\sigma(\mathbf{x}^k) \rightarrow \mathbf{u} \text{ as } k \rightarrow \infty \right\}. \end{aligned} \quad (\text{S5})$$

Points whose subdifferentials contains 0 are called (*limiting-critical points*).

Definition 6. (Kurdyka-Łojasiewicz (KL) Property) Let $\sigma : \mathbb{R}^d \rightarrow (-\infty, +\infty]$ be proper and lower semicontinuous.

(i) The function σ is said to have the Kurdyka-Łojasiewicz (KL) Property at $\bar{\mathbf{u}} \in \text{dom } \partial\sigma := \{\mathbf{u} \in \mathbb{R}^d : \partial\sigma(\mathbf{u}) \neq \emptyset\}$ if there exist $\eta \in (0, \infty]$, a neighborhood \mathcal{U} of $\bar{\mathbf{u}}$ and a function $\varphi \in \Phi_\eta$, such that for all

$$\mathbf{u} \in \mathcal{U} \cap [\sigma(\bar{\mathbf{u}}) < \sigma(\mathbf{u}) < \sigma(\bar{\mathbf{u}}) + \eta], \quad (\text{S7})$$

the following inequality holds

$$\varphi'(\sigma(\mathbf{u}) - \sigma(\bar{\mathbf{u}})) \text{dist}(0, \partial\sigma(\mathbf{u})) \geq 1. \quad (\text{S8})$$

(ii) If σ satisfies the KL property at each point of $\text{dom } \partial\sigma$, then σ is called a KL function.

It is shown in [Bolte et al., 2014] that KL functions arise in many applications for optimization, in particular, semi-algebraic functions are KL functions. The definitions for semi-algebraic function is given as follows.

Definition 7. (Semi-algebraic sets and functions). (i) A subset $\mathcal{S} \in \mathbb{R}^d$ is real semi-algebraic set if there exists a finite number of real polynomial functions $g_{ij}, h_{ij} : \mathbb{R}^d \rightarrow \mathbb{R}$ such that

$$\mathcal{S} = \cup_{j=1}^p \cap_{i=1}^q \{ \mathbf{u} \in \mathbb{R}^d : g_{ij}(\mathbf{u}) = 0 \text{ and } h_{ij}(\mathbf{u}) < 0 \}. \quad (\text{S9})$$

(ii) A function $h : \mathbb{R}^d \rightarrow (-\infty, +\infty]$ is called semi-algebraic if its graph

$$\{ (\mathbf{u}, t) \in \mathbb{R}^{d+1} : h(\mathbf{u}) = t \} \quad (\text{S10})$$

is a semi-algebraic subset of \mathbb{R}^{d+1} .

S.IV: PROOF OF GLOBAL CONVERGENCE OF ALGORITHM 1

In this section, we employ results from [Lin and Adetola, 2017], [Bolte et al., 2014] to analyze convergence of Algorithm 1. To simplify notation, we define $\tilde{g}(\mathbf{K}) \triangleq J(\mathbf{K}) + g(\mathbf{K})$, where $J(\mathbf{K})$ is the performance index of H_2 cost (10) and $g(\mathbf{K})$ is the indicator function for the H_∞ constraint (16).

Lemma 2: $\tilde{g} : \mathbb{R}^{m \times p} \rightarrow (-\infty, \infty]$ and $f : \mathbb{R}^{m \times p} \rightarrow (-\infty, \infty]$ are proper and lower semicontinuous functions.

Proof. In problem (18) the function $J(\mathbf{K})$ is the LQR cost when using the feedback gain \mathbf{K} . Clearly $f(\mathcal{K}) > -\infty$, and $J(\mathbf{K}) < +\infty$ if \mathbf{K} is stabilizing, thus function J is proper. In addition, $J(\mathbf{K})$ is continuous in \mathbf{K} [Rautert and Sachs, 1997], and therefore lower semicontinuous.

The function $g(\mathbf{K})$ in (16) is the indicator function for the level set $\mathcal{K}(\gamma)$ in (33), and thus can take either 0 or $+\infty$, with $g(\mathbf{K}) = 0$ whenever $\mathbf{K} \in \mathcal{K}(\gamma)$. Thus, $\tilde{g}(\mathbf{K})$ is proper. In addition, $g(\mathbf{K})$ is an indicator function of an open set, thus it is lower semicontinuous. Given J and g are both proper and lower semicontinuous, the summation $\tilde{g} = J + g$ is proper and lower semicontinuous. Similarly, $f(\mathbf{F})$ in (17) is a proper function. Moreover, it is shown in [Bolte et al., 2014] that it is lower semicontinuous. \square

Lemma 3: $H : \mathbb{R}^{m \times p} \times \mathbb{R}^{m \times p} \rightarrow \mathbb{R}$ is a continuously differentiable function, i.e., $H \in C^1$.

Proof. The gradient of $H(\mathbf{K}, \mathbf{F})$ (27) is continuous in \mathbf{K}, \mathbf{F} . Thus, $H \in C^1$. \square

Lemma 4: (i) $\inf_{\mathbb{R}^{m \times p} \times \mathbb{R}^{m \times p}} \Phi > -\infty$, $\inf_{\mathbb{R}^{m \times p}} f > -\infty$, and $\inf_{\mathbb{R}^{m \times p}} \tilde{g} > -\infty$, where Φ is given by (19).

(ii) The partial gradient $\nabla_{\mathbf{K}} H(\mathbf{K}, \mathbf{F})$ is globally Lipschitz with moduli $L_1(\mathbf{F})$, that is [Bolte et al., 2014],

$$\| \nabla_{\mathbf{K}} H(\mathbf{K}_1, \mathbf{F}) - \nabla_{\mathbf{K}} H(\mathbf{K}_2, \mathbf{F}) \| \leq L_1(\mathbf{F}) \| \mathbf{K}_1 - \mathbf{K}_2 \|.$$

Likewise, the partial gradient $\nabla_{\mathbf{F}} H(\mathbf{K}, \mathbf{F})$ is globally Lipschitz with moduli $L_2(\mathbf{K})$.

(iii) There exist bounds λ_i^-, λ_i^+ , $i = 1, 2$ such that

$$\begin{aligned} \inf \{ L_1(\mathbf{F}^k) : k \in \mathbb{N} \} &\geq \lambda_1^-, \inf \{ L_2(\mathbf{K}^k) : k \in \mathbb{N} \} \geq \lambda_2^- \\ \sup \{ L_1(\mathbf{F}^k) : k \in \mathbb{N} \} &\leq \lambda_1^+, \sup \{ L_2(\mathbf{K}^k) : k \in \mathbb{N} \} \leq \lambda_2^+ \end{aligned} \quad (\text{S11})$$

(iv) $\nabla H \triangleq (\nabla_{\mathbf{K}} H, \nabla_{\mathbf{F}} H)$ is Lipschitz continuous [Luenberger and Ye, 1984] on bounded subsets of $\mathbb{R}^{m \times p} \times \mathbb{R}^{m \times p}$. That is, for each bounded subset $\mathcal{B}_1 \times \mathcal{B}_2$ of $\mathbb{R}^{m \times p} \times \mathbb{R}^{m \times p}$ there exists $M > 0$, such that for all $(\mathbf{K}_i, \mathbf{F}_i) \in (\mathcal{B}_1, \mathcal{B}_2)$,

$$\begin{aligned} &\| \nabla_{\mathbf{K}} H(\mathbf{K}_1, \mathbf{F}_1) - \nabla_{\mathbf{K}} H(\mathbf{K}_2, \mathbf{F}_2) \|_F^2 \\ &+ \| \nabla_{\mathbf{F}} H(\mathbf{K}_1, \mathbf{F}_1) - \nabla_{\mathbf{F}} H(\mathbf{K}_2, \mathbf{F}_2) \|_F^2 \\ &\leq M (\| \mathbf{K}_1 - \mathbf{K}_2 \|_F^2 + \| \mathbf{F}_1 - \mathbf{F}_2 \|_F^2) \end{aligned} \quad (\text{S12})$$

Proof. (i)–(iv) are stated as assumptions in [Bolte et al., 2014]. We show that these assumptions hold for our sparsity-constrained mixed H_2/H_∞ problem. It is easy to see that (i) holds since f and g are indicator functions. Since J is the LQR performance index, $J(\mathbf{K}) > 0$. Thus $\tilde{g}(\mathbf{K}) > -\infty$. In (20), $H(\mathbf{K}, \mathbf{F}) \geq 0$, so $\Phi(\mathbf{K}, \mathbf{F}) > -\infty$. Properties (ii) and (iii) require the partial gradient of H to be globally Lipschitz, and the Lipschitz constant be upper and lower bounded, which is easy to verify since $L_1(\mathbf{F}^k) = L_2(\mathbf{K}^k) = \rho$ (27). Property (iv) holds since the left-hand side of (S12) can be expressed as: $LHS = 2\rho^2 \| (\mathbf{K}_1 - \mathbf{K}_2) - (\mathbf{F}_1 - \mathbf{F}_2) \|_F^2 \leq 4\rho^2 (\| \mathbf{K}_1 - \mathbf{K}_2 \|_F^2 + \| \mathbf{F}_1 - \mathbf{F}_2 \|_F^2)$. \square

Assumption 1: Function J is a semi-algebraic function [Bolte et al., 2014].

Lemma 5: The objective function Φ of (18) is a Kurdyka-Łojasiewicz (KL) function [Bolte et al., 2014].

Remark 1. A broad class of functions satisfy the semi-algebraic property, including polynomial functions, ℓ_0 -norm function and indicator function of positive semidefinite cones [Bolte et al., 2014]. The function $f(\mathbf{F})$ is the indicator function for the semi-algebraic set $\{ \mathbf{F} | \text{card}(\mathbf{F}) \leq s \}$. Thus, function f is semi-algebraic [Lin and Adetola, 2017], [Bolte et al., 2014]. The function $g(\mathbf{K})$ is the indicator function for the level set $\mathcal{K}(\gamma)$, which is approximated by the convex level set $\hat{\mathcal{K}}(\gamma_0)$, represented by the LMI (34), and $\hat{\mathcal{K}}(\gamma_0)$ is a semi-algebraic set [Netzer, 2016]. The coupling function H is polynomial, so it is semi-algebraic [Bolte et al., 2014]. Moreover, J is a semi-algebraic function by Assumption 1. Thus, each term of Φ is semi-algebraic, and since a finite sum of semi-algebraic functions is also semi-algebraic, Φ is semi-algebraic. It is shown in Theorem 5.1 in [Bolte et al., 2014] that a semi-algebraic function satisfies the KL property at any point in its domain. Thus, Φ is KL.

It has been proved in [Bolte et al., 2014] that if Lemma 2–4 hold, then the sequence generated by PALM algorithm globally converges. In addition, if Lemma 5 holds, the sequence converges to a critical point [Bolte et al., 2014] of Φ . This confirms convergence of Algorithm 1 to a sparsity-constrained mixed H_2/H_∞ controller, which corresponds to a critical point of Φ under mild assumptions on the functions J and g .

REFERENCE

- [Bazaraa et al., 2013] Bazaraa, M. S., Sherali, H. D., and Shetty, C. M. (2013). *Nonlinear programming: theory and algorithms*. John Wiley & Sons.
- [Bolte et al., 2014] Bolte, J., Sabach, S., and Teboulle, M. (2014). Proximal alternating linearized minimization or nonconvex and nonsmooth problems. *Mathematical Programming*, 146(1-2):459–494.
- [Lin and Adetola, 2017] Lin, F. and Adetola, V. (2017). Co-design of sparse output feedback and row/column-sparse output matrix. In *American Control Conference (ACC), 2017*, pages 4359–4364. IEEE.
- [Luenberger and Ye, 1984] Luenberger, D. G. and Ye, Y. (1984). *Linear and nonlinear programming*, volume 2. Springer.
- [Netzer, 2016] Netzer, T. (2016). Real algebraic geometry and its applications. *arXiv preprint arXiv:1606.07284*.
- [Rautert and Sachs, 1997] Rautert, T. and Sachs, E. W. (1997). Computational design of optimal output feedback controllers. *SIAM Journal on Optimization*, 7(3):837–852.